Spores from the K–Pg boundary of the La Colonia Formation, Patagonia, Argentina.

Facundo De Benedetti[a,b,*], María C. Zamaloa[b], María A. Gandolfo[b,c], Néstor R. Cúneo[b]

[a] Consejo Nacional de Investigaciones Científicas y Técnicas (CONICET)

[b] Museo Paleontológico Egidio Feruglio, Avenida Fontana 140, 9100 Trelew, Chubut, Argentina

[c] L. H. Bailey Hortorium, Plant Biology Section, School of Integrative Plant Science, Cornell University, Ithaca, New York 14853, USA

[*] Corresponding author

E-mail addresses: fdebenedetti@mef.org.ar (F. De Benedetti), mzamaloa@gmail.com (M.C. Zamaloa), magandolfo@cornell.edu (M.A. Gandolfo), rcuneo@mef.org.ar (N.R. Cúneo).

Abstract

A palynological study was carried out based on 157 samples collected from four representative stratigraphic sections of the Maastrichtian-Danian deposits of the La Colonia Formation outcropping in northern Chubut Province, Patagonia, Argentina. About 240 palynomorphs were recognized. Plant communities were dominated in terms of richness by ferns and angiosperms, but algae and gymnosperms are also well-represented. In this contribution, we present the systematic study of bryophyte, lycophyte, and fern spores. Bryophytes comprise eight species (10% of spore diversity), including representatives of Marchantiophyta, Bryophyta, and Anthocerotophyta. Lycophytes encompass 15 species (20% of spore diversity) and are represented by the families Lycopodiaceae and Selaginellaceae. Ferns comprise 53 species (70% of spore diversity), including members of Anemiaceae, Dicksoniaceae, Dipteridaceae, Gleicheniaceae, Lygodiaceae, Marsileaceae, Matoniaceae, Osmundaceae, Polypodiaceae, Salviniaceae, and Schizaeaceae, among others of uncertain affinities. Four new species are erected: a lycophyte (*Neoraistrickia loconiensis* sp. nov.), a salvinialean (*Thecaspora*

polygonalis sp. nov.), and two fern species of unknown affinities (*Clavatosporis varians* sp. nov. and *Microreticulatisporites patagonicus* sp. nov.). The recorded palynoflora reinforces previous environmental interpretation of the La Colonia deposits as coastal plains bathed by shallow seas and barrier island/lagoon complexes and the presence of freshwater bodies where aquatic plant communities developed. The vegetational history of the bryophytes, lycophytes, and ferns in the studied sections of the La Colonia Formation indicates the lack of a significant floristic change across the K-Pg interval at the local scale.

Keywords: Bryophytes; Lycophytes; Ferns; K–Pg boundary; Palynology; Patagonia.

1. INTRODUCTION

The La Colonia Formation (Maastrichtian-Danian) outcropping at the central north of the Chubut Province, Patagonia, Argentina, comprises one of the most diverse terrestrial biotas from the Late Cretaceous of South America (Fig. 1). The presence of freshwater green algae (e.g., Cúneo et al., 2014), water ferns (e.g., Cúneo et al., 2013; De Benedetti et al., 2018, 2020, 2021; Hermsen et al., 2013, 2019), a species of the free-floating Araceae clade (Gallego et al., 2014), Nelumbonaceae (Gandolfo and Cúneo, 2005), and Typhaceae (Cúneo et al., 2021) revealed the occurrence of wetland communities in a diverse freshwater to brackish paleoecosystem thriving in warm to warm-temperate and humid climatic conditions (Cúneo et al., 2014, 2021). The fauna that prospered at La Colonia includes dinosaurs, terrestrial and freshwater turtles, crocodiles, plesiosaurs, fishes, snakes, birds, mammals, ostreid bivalves, foraminifera, and water bugs, among others (e.g., Cúneo et al., 2014; Oriozabala et al., 2020; Panzeri et al., 2020; O'Gorman, 2021).

The Cretaceous-Paleogene (K-Pg) mass extinction event (~ 66 Ma) is believed to have been caused by the environmental effects of the collision of an extraterrestrial bolide on the Yucatan Peninsula in southern Mexico (Raup and Sepkoski, 1982; Schulte et al., 2010). Approximately

75% of marine species and similar numbers of land animals become extinct in a geologic instant (Jones et al., 2023; Wilf et al., 2023). Plants show very different extinction patterns from animals, with a sharp contrast between high-resolution regional stratigraphic studies, which usually show significant plant-species extinction, and global syntheses or phylogenetic analyses, which show no losses of plant families or major clades (e.g., Nichols and Johnson, 2008; Stiles et al., 2020; Thompson and Ramírez- Barahona, 2023; Wilf et al., 2023). Additionally, contrasting results from palynological and macrofloral data and phylogenetic analyses have led to a debate regarding whether there was any significant K-Pg extinction for plants (e.g., Thompson and Ramírez- Barahona, 2023; Wilf et al., 2023).

According to Wilf et al. (2023), two main plant-relevant factors promote global heterogeneity in the effects of the K-Pg extinction. These are the distance to the Chicxulub crater and the maritime and latitudinal buffering of the impact winter (Bardeen et al., 2017; Brugger et al., 2017; Morgan et al., 2022). Both distance and buffering gradients predict large extinctions in western North America and the Neotropics and less severe extinctions in the maritime areas of temperate Gondwana (Wilf et al., 2023).

Interestingly, a worldwide palynological event, known as the fern-spore spike, is a distinctive feature of the K-Pg boundary, and it is recorded at a single stratigraphic interval that can be as thin as 1 cm (Vajda and Bercovici, 2014; Berry, 2023). This spike is detected when fern spores are anomalously abundant within or immediately above the boundary clay (Orth et al., 1981; Tschudy et al., 1984; Berry, 2023) and has been recorded in geographically distant regions such as North America (Berry, 2023), Japan (Saito et al., 1986), and New Zealand (Vajda et al., 2001, 2004; Vajda and Raine, 2003). In South America, north of the Equator, a fern spike has been recorded in Gorgonilla Island, Colombia (Renne et al., 2018; Bermúdez et al., 2019). In southern South America, specifically in Patagonia, a fern-spore spike has not been recorded yet; nonetheless, a similar "*Classopollis* pollen spike" was recorded at Danian levels of the Lefipán Formation (Barreda et al., 2012), and it has later been recorded in several localities

around the world, such as in China and Borneo (e.g., Berry, 2022a, 2022b). Although no *Classopollis* spike was detected in the La Colonia Formation (Clyde et al., 2021), this pollen remains anomalously abundant across the K-Pg boundary relative to other K-Pg boundary sections globally (Berry, 2022a).

Here, we report the systematic treatment of bryophyte, lycophyte, and fern spores and their paleoenvironmental input during the K-Pg floral transition from the palynological study carried out from samples collected at four localities of the La Colonia Formation in the Arroyo Mirasol Chico Creek area (Fig. 1). We have previously presented the taxonomic treatment of the gymnosperms and angiosperm components of the La Colonia Formation in De Benedetti et al. (2023a).

2. MATERIALS AND METHODS

2.1. Geological setting, specimen sampling, preparation, and curation

Stratigraphically, the La Colonia Formation overlies the fluvial deposits of the Campanian-Maastrichtian Puntudo Chico Formation (Ardolino and Franchi, 1996; Anselmi et al., 2004). Overlying units include brackish paludal siliciclastic facies of the Paleocene Cerro Bororó Formation, the Paleocene-Eocene El Buitre Formation basalts, and Oligocene pyroclastic rocks of the Sarmiento Formation (Ardolino and Franchi, 1996; Anselmi et al., 2004; Sacomani et al., 2007). Biostratigraphic estimates (Malumián et al., 1991; Ardolino and Franchi, 1996; Page et al., 1999; Náñez and Malumián, 2008; Guler et al., 2014) and recent paleomagnetic analyses (Clyde et al., 2021) support a Maastrichtian to Danian age for the La Colonia deposits.

A total of 157 samples were collected from four stratigraphic sections: 1- Quebrada del Helecho/Cañadón del Irupé (QH/CI), 2- Cerro Bosta (CBO), 3- Cerro Buitre Norte (CBN = Plesiosaurio locality 'LCP' of De Benedetti et al., 2021), and 4- Chiva Muerta (CHM) (Fig. 1). The K-Pg boundary was recognized in the Cerro Buitre Norte section based on magnetostratigraphic and palynological data provided in Clyde et al. (2021). The other three

sections (QH/CI, CBO, CHM) are interpreted as Maastrichtian in age throughout (De Benedetti et al., 2023a).

The samples were processed using standard palynological techniques (Traverse, 2007). Light microscope (LM) observations were made with a Nikon Eclipse 80i microscope coupled with a Nikon DS-L4 camera (Nikon Corp., Minato, Tokyo, Japan) at the Museo Paleontológico Egidio Feruglio (MEF) Trelew, Chubut Province, Argentina. Coordinates of each photographed palynomorph correspond to the mentioned microscope. Scanning electron microscope (SEM) observations were made with a desktop Phenom XL at the L.H. Bailey Hortorium, Cornell University, Ithaca, New York, U.S. Images were edited using Adobe Photoshop CS6. Microscope slides and SEM stubs are housed at the Museo Paleontológico Egidio Feruglio palynological collection under the repository acronyms MPEF-PA 125–999.

3. RESULTS

Of the 157 samples, only 83 were palynologically productive, and about 240 palynotaxa were identified. Plant communities were dominated in terms of richness by ferns and angiosperms, but algae and gymnosperms are also well-represented (Clyde et al., 2021; De Benedetti et al., 2023a). Among the spores, eight belong to bryophytes, 15 to lycophytes, and 53 to ferns (Table 1).

……INSERT TABLE 1 HERE……..

New spore species and those specimens that provide valuable information to previously published species are described below. Elements commonly found in Patagonian palynofloras and those that could only be assigned at the generic level (either because of their poor preservation and/or because of the few specimens recovered) are only illustrated. Some species with different taxonomic assignments mentioned in Clyde et al. (2021) are listed in Appendix A.

130 *3.1. Systematic palynology*

131 BRYOPHYTES

132 *Family:* RICCIACEAE Reichenbach 1828

133 *Genus:* **Zlivisporis** Pacltová 1961

134 *Type species: Zlivisporis blanensis* Pacltová 1961

135 *Zlivisporis asper* (Srivastava) De Benedetti comb. nov.

136 Plate I, Fig. 5

137 *Basionym: Triporoletes asper* Srivastava, in Srivastava (1972), Palaeontographica Abteilung B,

138 139 (1–4), p. 34.

139 *Remarks:* Braman (2001) argued cogently that *Zlivisporis* can be separated from *Triporoletes*

140 Mtchedlishvili in Mtchedlishvili and Samoilovitch 1960, based on the morphology of the type

141 species. Following Braman (2001), *Triporoletes asper* is here transferred to *Zlivisporis*.

142 *Distribution:* The species has a wide geographic and stratigraphic distribution ranging from

143 Mesozoic to early Cenozoic deposits of North and South America, Europe, and Asia (e.g.,

144 Srivastava, 1972; Song et al., 1999; Yi and Batten, 2002; Papú, 2002; Palynodata Inc. and

145 White, 2006; Saxena and Tripathi, 2012).

146 *Botanical affinity: Riccia* L. (Srivastava, 1972).

147

148 LYCOPHYTES

149 *Family:* SELAGINELLACEAE Willk. 1854

150 *Genus:* **Acylomurus** Paden Phillips in Paden Phillips and Félix 1971

151 *Type species: Acylomurus sejunctus* Paden Phillips and Félix 1971

152 *Acylomurus silviae* Perez Loinaze et al. 2023

153 Plate I, 29 and 30; Plate II, Figs. 1–8

154 *Description:* Spores trilete, with a subcircular to convex subtriangular amb. Laesurae straight or

155 sinuous, extended to the equatorial margin but often obscured by the sculpture and thus

appearing shorter, bordered by membranous lips of 2–3 µm high (Plate I, 29, 30). Exine two-layered. Nexine thin and psilate, ~ 1 µm thick, forming a distinct central body (Plate I, 29, 30). Sexine up to 11 µm thick, thinner proximally and thicker towards the equator and distally forming a patina that is crossed by “channels” or incisions that delimit “islands” (verrucae and rugulae) of sexine of variable sizes (Plate I, 29, 30; Plate II, 1, 2). In several specimens the nexine is separated from the sexine distally forming a cavate structure and is sometimes folded (Plate I, 30). Distal face and equatorial margin ornamented with coni and echinae ~ 0.5–2.0 µm high and up to 1.5 µm wide at the base (Plate II, 1, 2, 6, 7). Proximal sculpture less developed or absent. Usually occurring as tetrahedral tetrads (Plate II, 3–6).

Dimensions: Equatorial diameter 24 (38) 63 µm (42 specimens); central body 24 (30) 47 µm (14 specimens); tetrads 43 (62) 85 µm (7 specimens).

Studied material: MPEF-PA 151, 168, 171, 577, 692, 701, 752, 819, 925–928, 930, 942, 944, 951, 966.

Occurrence: Sections CBO, CBN.

Remarks: This species was recently described at the Maastrichtian of the Chorrillo Formation, Austral-Magallanes Basin, southern Patagonia, Argentina (Perez Loinaze et al., 2023). As indicated by Perez Loinaze et al. (2023), it displays a high morphological variation in the grade of fusion of the verrucae and in the density of the suprasculpture. Specimens from the La Colonia are distinguished from those from the Chorrillo Formation only by having more strongly fused verrucae. The spores of *A. silviae* also occur usually as tetrahedral tetrads (Plate II, 3–6) as mentioned for the type species (Paden Phillips and Félix, 1971). Tetrads are composed of spores that have similar or different dimensions. Interestingly, some of them have a smaller cavate spore, with a reduced sculpture and without the characteristic patina of the species, which would be better placed in *Lusatisporis choiols* Perez Loinaze et al. (Plate II, 3–5), which was also recently described for the Maastrichtian of the Chorrillo Formation (Perez Loinaze et al., 2023). Both forms were commonly found dispersed in the La Colonia palynological slides;

although those like *A. silviae* (Plate I, 29, 30) were proportionally more abundant than those like *L. choiols* (Plate II, 8), also suggesting that both morphotaxa were probably produced by the same natural species. We prefer to retain all these specimens in *A. silviae* as *L. choiols* is apparently an abortive/anomalous form.

Botanical affinity: Similar forms to *A. silviae* and *L. choiols* are found in *Selaginella* Beauvois (e.g., Zhou et al., 2015).

Genus: **Neoraistrickia** Potonié 1956

Type species: Neoraistrickia truncatus (Cookson) Potonié 1956

Neoraistrickia loconiensis De Benedetti and Zamaloa sp. nov.

Plate II, Figs. 17–23

1973. *Neoraistrickia* sp., in Archangelsky (1973), Ameghiniana, 10(4), Lam. 1, figs. 7 and 8.

2023. *Baculatisporites kachaikensis* Llorens and Archangelsky, in Perez Loinaze et al. (2023), Review of Palaeobotany and Palynology, 314, 104893, pl. 1, fig. 8.

Etymology: The epithet “loconiensis” is an anagram derived from coloniensis, the name of the formation from which the specimens come.

Type locality: Cerro Buitre Norte locality, La Colonia Fm., Chubut Province, Argentina.

Holotype: MPEF-PA 923 (Plate II, 17).

Paratype: MPEF-PA 924 (Plate II, 18).

Additional material: MPEF-PA 145, 147, 149, 274, 150, 168–172, 454, 457, 652, 655, 678, 680, 690–692, 752, 753, 793, 821, 826, 827, 835, 870, 922–925, 928, 952.

Stratigraphic horizon: La Colonia Formation, Maastrichtian to early Danian.

Diagnosis: Spore trilete, amb triangular to subcircular. Laesurae about 3/4 spore radius or reaching to margin, with raised lips. Exine two-layered, inner ~ 1 µm thick, outer sculptured with bacula, coni, spines, and verrucae. Sculptural elements 1.5–4.5 µm high, densely to sparsely

placed, fused at the base, sometimes forming an irregular microfoveolate surface. Tip of the elements usually truncate and with multiple papillae.

Description: The amb is highly variable, ranging from triangular to rounded triangular to subcircular (Plate II, 17–23). The laesurae has raised membranous lips of up to 1.5 µm high (Plate II, 20 and 22). The exine is sculptured with slender to robust bacula, coni, spines, and verrucae, densely to sparsely arranged. Some specimens have mostly bacula of relatively similar sizes and shapes (Plate II, 17 and 20), and others have mostly conical and baculate/verrucate elements (Plate II, 18, 19, 21, 22), but all of them tend to have truncate apices that are commonly divided into multiple papillae (Plate II, 23). The sculptural elements are 1.5 to 3 µm high, rarely up to 4.5 µm, fused at the base and occasionally forming an irregular microfoveolate surface (Plate II, 21).

Dimensions: Maximum equatorial diameter 17 (32) 48 µm (62 specimens).

Occurrence: Sections QH/CI, CBO, CBN, CHM.

Comparisons: N. loconiensis differs from most other species of *Neoraistrickia* in having sculptural elements with the tips minutely dissected into multiple terminal papillae. The type species *N. truncatus* from the Upper Mesozoic of Australia has scattered bacula (Cookson, 1953; Dettmann, 1963). *N. robusta* Brenner from the Lower Cretaceous of USA is larger and has larger sculptural elements (Brenner, 1963). The most similar species is apparently *N. speciosa* Srivastava from the Maastrichtian of Canada, it matches in size and sculpture, but has a distal Y-shaped crassitude (Srivastava, 1972).

Distribution: Argentina, Patagonia, Maastrichtian (Perez Loinaze et al., 2023) and Paleocene (Archangelsky, 1973).

Botanical affinity: Similar forms are found in *Selaginella* (e.g., Zhou et al., 2015).

FERNS

Class: POLYPODIOPSIDA Cronquist, Takht. and W. Zimm. 1966

Order: SALVINIALES Link 1833

Family: MARSILEACEAE Mirbel 1802

Molaspora lobata (Dijkstra) Hall, in Hall and Peake 1968 / *Crybelosporites pannuceus* (Brenner) Srivastava 1977

Plate III, Figs. 22 and 23

Remarks: Both species were described in De Benedetti et al. (2021). Here we illustrate for the first time the microspores (*C. pannuceus*) attached to the megaspores (*M. lobata*), strongly suggesting that both taxa were produced by the same species.

Molaspora reticulata Campbell and Untergasser 1972 / *Gabonisporis cristata* (Stanley) Sweet 1986

Plate III, Figs. 24–30

Remarks: Both species were described in De Benedetti et al. (2021). Here we illustrate for the first time the microspores (*G. cristata*) attached to the megaspores (*M. reticulata*), strongly suggesting that both taxa were produced by the same species.

Family: SALVINIACEAE Martinov 1820

Genus: **Azolla** Lamarck 1783

Type species: Azolla filiculoides Lamarck 1783

Azolla andreisii De Benedetti and Zamaloa 2021

Plate IV, Figs. 1–18

Expanded description: Megaspore apparatus oval to elliptical, composed of a spherical to subspherical megaspore and a float apparatus situated proximally (Plate IV, 1–8). The megaspore surface is completely covered by perinal hairs (c. 0.3–2.0 µm diameter), while the float apparatus is scarcely covered by hairs. Megaspore wall composed of a homogeneous exine (c. 8–12 µm thick) and a two-layered perine (c. 5–20 µm thick) (Plate IV, 20 and 21). The

differentiation between endo- and exoperine is obscure; the endoperine is 4–12 µm thick and has a granular appearance and a dense pseudovacuolated structure (with the alveoli almost indistinguishable); the exoperine constitutes a very thin and homogeneous layer c. 0.5 µm thick from which small papillae and granula (up to 1.4 µm long) emerge (Plate IV, 9 and 10). Megaspore surface with tubular to conical protuberances or perinal excrescences (c. 20–40 µm long x 11–16 µm wide at the base) (Plate IV, 9–13). The papillate elements are larger in the protuberances, and are usually reduced or absent towards their tips, which are occasionally flat, striate, and punctate (Plate IV, 13). The perinal hairs that cover the megaspore surface emerge from the proximal pole of the megaspore and not from the megaspore surface; therefore, there is no infrafilosum.

The float apparatus is composed of c. 18 to more than 30 pseudovacuolate floats arranged in three to five poorly defined tiers (Plate IV, 1–3), sometimes placed in three well defined compartments (Plate IV, 4–6). The floats are of variable shape (rhombic, elliptic, quadrangular, to irregular) and size (87–237 µm). The upper level comprises probably only three floats, while the lowermost level is usually the most numerous, with smaller floats covering part of the megaspore body. Sometimes, smaller floats (30 to 50 µm) are interspaced. The floats have a rough surface, sometimes with fused wrinkles forming an irregular reticulum or defining a concentric wavy pattern (Plate IV, 14), but occasionally granulate/papillate (Plate IV, 15). The inner surface of the floats develops numerous extensions that narrow distally to form long perinal hairs (Plate IV, 16). In a single specimen, long perinal hairs with circinate/coiled tips emerge between the floats (Plate IV, 17 and 18).

Dimensions: Length of megaspore apparatus 481 (639) 778 µm, width of megaspore apparatus 306 (411) 545 µm (22 specimens measured); diameter of megaspore 237 (302) 340 µm (three specimens measured).

Occurrence: Sections, CBO, CBN.

Azolla coloniensis De Benedetti and Zamaloa emend. Hermsen et al. 2019

Plate IV, Figs. 19–26

Expanded description: Megaspore apparatus oval to elliptical, composed of a spherical to subspherical megaspore and a float apparatus situated proximally (Plate IV, 19–22). The megaspore surface is completely covered by perinal hairs (c. 0.4–1.0 μm in diameter), while the float apparatus is usually partially visible below the hairs. Megaspore wall is composed of a homogeneous exine and a two-layered perine (endoperine and exoperine) from which perinal hairs emerge. The perine is morphologically variable. Most specimens have a relatively homogeneous perine (Plate IV, 19; as was described in De Benedetti et al., 2018). Other specimens have tuberculate perinal excrescences (c. 15–30 μm wide and up to 23 μm long) (Plate IV, 21 and 22), and there are transitional forms with the excrescences obscured by compression and the dense mat of hairs (Plate IV, 20). The perinal hairs emerge between and from the contours of the excrescences (Plate IV, 23).

The float system extends over the proximal surface of the megaspore and consists of 18–21 or more floats arranged in three or sometimes four tiers. The floats are variable in shape and size (c. 50–150 μm) and have a pseudovacuolate structure. The perine forms a tripartite columella that extends proximally through the float system and covers the trilete laesurae of the megaspore and hairs arise from this to enmesh the floats (Plate IV, 24).

The microspore massulae were found attached to the megaspore apparatuses (Plate IV, 19). The massulae have anchor-shaped glochidia (Plate IV, 25) and the microspores are microgranulate or microverrucate (Plate IV, 26).

Dimensions: Length of megaspore apparatus 304 (411) 522 μm (43 specimens measured); width of megaspore apparatus 176 (271) 360 μm (47 specimens measured); diameter of megaspore ca. 160–320 μm; diameter of microsporangium 129 (180) 223 μm (38 specimens measured); maximum length of microspore massulae 55 (87) 178 μm (51 specimens measured); diameter of microspore 11 (21) 30 μm (80 specimens measured).

311 *Occurrence:* Sections QH/CI, CBO, CBN, CHM.

312 *Comments:* Vegetative remains in organic connection with the reproductive structures were

313 described in Hermsen et al. (2019).

314

315 *Azolla* sp. cf. *A. keuja* Jud, De Benedetti, Gandolfo, and Hermsen 2019

316 Plate IV, Figs. 27–30; Plate V, 1–10

317 *Description:* The megaspore apparatus is oval to elliptical, composed of a spherical to

318 subspherical megaspore and a float apparatus situated proximally (Plate IV, 27–30). The float

319 apparatus is completely covered by perinal hairs (c. 0.2–3.0 µm in diameter), while the

320 megaspore surface lacks hairs. The megaspore wall is composed of a homogeneous exine (c.

321 3.0–3.5 µm thick) and a two-layered perine (c. 12–20 µm thick) (Plate V, 1, 2). The endoperine

322 is variable in thickness c. 1–7 µm thick, has a pseudovacuolated structure, and is expanded in

323 the raised areas of the excrescences (Plate V, 1). The exoperine is 3–6 µm thick (sometimes

324 more reduced in the tips of the excrescences), composed of a thin columellate layer of up to 0.8

325 µm thick and a solid tectate layer c. 2.5–5.5 µm thick (Plate V, 1 and 2).

326 The megaspore surface is covered by numerous irregularly distributed perinal excrescences.

327 The excrescences are highly variable in shape and size (5–65 µm in maximum width) (Plate IV,

328 27–30), sometimes larger at the distal pole (Plate IV, 28). Occasionally, the ornamentation

329 consists of folds or rugulae (Plate IV, 29), but in other cases, the sculpture is only composed of

330 small tuberculate/verrucate excrescences (Plate IV, 30). At the apexes of the excrescences, the

331 solid tectate layer of the exoperine is reduced, and it usually grades to free smaller or partially

332 fused clavae and granules (ca. 0.8–2.6 µm diameter and up to 2 µm high) (Plate V, 3 and 4).

333 Other parts of the excrescences, and the spaces between, are usually ornamented with rugulae,

334 granules, or verrucae (ca. 1–5 µm in diameter) (Plate V, 3), but not always (Plate V, 4). A fine

335 irregular reticulum, composed of very thin ridges (ca. 0.05 µm wide), is sometimes present in

336 the exoperine surface, occasionally with additional microgranules (ca. 0.1–0.3 µm diameter)

(Plate V, 5). Perinal hairs were not found on the surface of the megaspore; therefore, there is no infrafilosum.

The float system occupies the proximal two-fifths to proximal half of the megaspore apparatus. The float apparatus is thimble-shaped, and in almost all the specimens analyzed, the floats are not clearly delimited, and the perinal hairs cover them almost completely (Plate IV, 27, 29). Sometimes the float apparatus is covered by remains of the indusial cap (Plate IV, 28). There is a central tripartite columella with a variety of sculptural elements, such as granules, clavae, verrucae, and rugulae, from which hairs arise to attach the floats (Plate V, 7 and 8). A collar that forms a relatively homogeneous ring subtends the floats (Plate IV, 27), although it is sometimes poorly defined (Plate IV, 29, 30). The collar originates from the perine in the proximal region of the megaspore. The floats have a vacuolated structure (Plate IV, 30; Plate V, 6, 8, 9) and are completely covered by the hairs (0.2–3.0 µm diameter) of the suprafilosum (Plate V, 6). The floats are attached by perinal hairs that mostly arise from the inner surface of the collar and the columella, but also from hairs that emerge from the inner surface of the floats (Plate V, 7–10). In most cases, the surface of the collar has the same sculpture as those of the excrescences (i.e., small clavae, granules, and verrucae). The number of floats is uncertain; six floats arranged in one tier were counted in one specimen (Plate IV, 30), although more than nine were probably present in others (Plate V, 8, 9).

Dimensions: Length of megaspore apparatus 199 (286) 351 µm (13 specimens measured), width of megaspore apparatus 153 (216) 272 µm (30 specimens measured).

Occurrence: Section CBN.

Comments: This species is notably similar to *Azolla keuja* from the Danian of Salamanca Formation, which also outcrops in Chubut, Patagonia (Hermsen et al., 2019). Only minor differences were found between them, such as in size (up to 410 µm in *A. keuja*) and the collar's development (less conspicuous in *A. keuja*). Unfortunately, in both species, the float apparatus is not clearly defined to make better comparisons, and no microspore massulae were found

attached to the megaspores of the La Colonia specimens. Notably, similar megaspores were also reported as *Azolla* sp. 1 from the Maastrichtian of Lago Colhué Huapi Formation that outcrops near the La Colonia and Salamanca formations (Vallati et al., 2017). These megaspores were described based on few poorly preserved specimens. Still, it is quite possible that all of them (La Colonia, Salamanca, and Lago Colhué Huapi) were produced by the same species.

Family: INCERTAE SEDIS

Genus: **Azollopsis** Hall 1968 emend. De Benedetti and Zamaloa 2021

Type species: Azollopsis coccoides Hall 1968 emend. Sweet and Hills 1974

Azollopsis intermedia Sweet and Hills 1974

Plate V, Figs. 12–14

Remarks: This species was first described in the Late Cretaceous of North America (Sweet and Hills, 1974), and it was also described for the La Colonia Fm. in De Benedetti et al. (2021). Here we illustrate a complete microsporangiate sori comprising about ten microsporangia (Plate V, 12), but several other fragmented microsporangiate sori with about 10 to probably more than 15 microsporangia, reaching up to 910 µm in maximum length, were also recorded. The exine of the microspore was previously described as microgranular (De Benedetti et al. 2021, p. 9) but can also be psilate (Plate V, 13) or microgranulate/punctate (Plate V, 14). The exine thickness is 0.9–1.4 µm, and the laesurae has conspicuous lips (Plate V, 13 and 14).

Azollopsis tomentosa Hall 1968

Plate V, Figs. 15 and 16

Remarks: This species was first described in the Late Cretaceous of North America (Sweet and Hills, 1974), and it was also described for the La Colonia Fm. in De Benedetti et al. (2021). Here we illustrate the microspore massulae attached to the megaspore apparatus for the first time.

Genus: **Thecaspora** Elsik 1966

Type species: Thecaspora spinosa Elsik 1966

Thecaspora polygonalis De Benedetti sp. nov.

Plate V, Figs. 17–23

Etymology: Referring to the polygonal reticulum.

Type locality: Cerro Buitre Norte locality, La Colonia Fm., Chubut Province, Argentina.

Holotype: MPEF-PA 767 (Plate V, 17 and 18)

Paratypes: MPEF-PA 766 (Plate V, 19 and 20)

Additional material: MPEF-PA 381, 691, 766, 767, 772, 844, 944, 976.

Stratigraphic horizon: La Colonia Formation, Maastrichtian to early Danian.

Diagnosis: Microspore trilete, spheroidal to elliptical. Proximal acrolamella membranous, trirradiate. Exine 0.5–1.0 µm thick. Perine psilate, membranous, with spines ca. 3–8 µm long, interconnected by muri, forming a reticulum of triangular to polygonal lumina. Muri low and thin to high and membranous. Borders of acrolamella and membranous muri psilate or with small spiniform processes.

Description: The microspores are trilete, spheroidal to elliptical, with a proximal membranous trirradiate acrolamella (Plate V, 17–21). The laesurae extends 3/4 or the entire spore radius (Plate V, 18, 20, 23). The acrolamella is of very variable size, ca. 4–16 µm high and 18–33 µm wide. The wall is composed of exine and perine. The exine is 0.5–1.0 µm thick, and it is covered by a thin psilate membranous perine that is modified locally into spines ca. 3–8 µm long. The spines are conical and hollow at the base, and they are interconnected by muri or ridges forming a regular reticulum with polygonal lumina ca. 3–7 µm diameter. The muri are low and

thin to high and membranous. The borders of the acrolamella and membranous muri usually have small spiniform processes ca. 0.5–2.0 µm long. In some specimens, the processes are reduced, and the interconnected membranous muri with serrate margins constitute the most conspicuous sculptural elements. Several clusters of microspores were also recorded, probably part of the microsporangia content (Plate V, 22 and 23). The number of microspores per microsporangia is uncertain, but at least 30 have been counted.

Dimensions: Total length: 23 (31) 40 µm (29 specimens measured); total width: 26 (31) 39 µm (8 specimens measured); microspore diameter: 14 (18) 22 µm (54 specimens measured); maximum diameter of microsporangia remain: 79 (101) 124 µm (6 specimens measured).

Occurrence: Sections QH/CI, CBO, CBN, CHM.

Remarks: Elsik (1966) established *Thecaspora* to describe microspores with acrolamella ("trifolium" in Elsik) and spinose ornamentation. Hills (1967), Gunther and Hills (1970), and Singh (1983) considered *Thecaspora* as a synonym of *Ariadnaesporites*. As Batten and Kovach (1990) indicate, the placement of *Thecaspora* in synonymy with *Ariadnaesporites* is questionable. In this work, the generic name *Thecaspora* is taken up again, considering that it is distinguished from *Ariadnaesporites* because it lacks elongated distal processes (Tschudy, 1966), and from *Ghoshispora* Srivastava emend. Dettmann because of the absence of a secondary sculpture between the mural and/or spinose projections (Dettmann, 1995). *Balmeisporites* Cookson and Dettmann emend. Dettmann has a prominent reticulum in each equatorial radial region and lacks spinose ornamentation (Dettmann, 1995).

Comparisons: T. spinosa from the Campanian of Perú is larger (60–80 µm length) and has larger processes (10–20 µm long) (Elsik, 1966). *T. lacrimata* de Jersey from the Triassic of Australia is the only other species included in the genus, and it is also larger (50–86 µm length), lacks a reticulum, and has smaller apiculate sculpture (de Jersey, 1979).

Genus et species indet.

Plate V, Figs. 24 and 25

Description: Microspore massula with irregular outline and a pseudovacuolate structure containing 1 to 6 trilete microspores. Surface with sparsely distributed aseptate glochidia of 12–36 µm long. Glochidia with rhombic to scythe-shaped tips. Microspores spherical to elliptical, laesurae extended 3/4 or the entire spore radius. Exine 0.5–1.0 µm thick, psilate.

Dimensions: Massulae: 37 (50) 86 µm diameter (8 specimens); microspore: 13 (19) 23 µm diameter (15 specimens).

Studied material: MPEF-PA 381, 396, 766, 767.

Occurrence: Sections QH/CI, CBN, CHM.

Remarks: Microspore massulae with similar glochidia has been described in the modern *Azolla pinnata* R.Br. and *Azolla nilotica* Decne. ex. Mett. (Strasburger, 1873), but also in *Azolla danica* Bertelsen from the Lower Pleistocene of Denmark (Bertelsen, 1972). However, as there are several fossil genera that also produced microspore massulae with glochidia (e.g., *Paleoazolla* and *Azollopsis*), we prefer to leave this species with open nomenclature until we have more information about its megaspores.

Order: INCERTAE SEDIS

Family: INCERTAE SEDIS

Genus: **Clavatosporis** Song and Zhong 1984

Type species: Clavatosporis baculus Song and Zhong 1984

Clavatosporis varians De Benedetti sp. nov.

Plate VI, Figs. 9–12

Etymology: Referring to the variety of sculptural elements.

Type locality: Cerro Buitre Norte locality, La Colonia Fm., Chubut Province, Argentina.

Holotype: MPEF-PA 828 (Plate VI, 9)

Paratype: MPEF-PA 927 (Plate VI, 10).

Additional material: MPEF-PA 628, 828, 863, 873, 927, 928, 946, 955, 962, 989.

Stratigraphic horizon: La Colonia Formation, Maastrichtian to early Danian.

Diagnosis: Spore monolete, amb elliptical. Laesura about 3/4 spore length. Exine 1.0–1.5 µm thick, echinate/baculate. Spines and bacula up to 4.5 µm high and 1.1 µm wide, sparse to densely distributed. Small granules, coni, and verrucae are frequently interspaced.

Description: The spores are monolete, bean-shaped in lateral view and elliptical in polar view. The laesura is straight, extended 3/4 the spore length, simple or with a weak margo. The exine is 1.0–1.5 µm thick. The sculpture is composed of spines and bacula of 1.0–4.5 µm high and 0.5–1.1 µm wide, sparse to densely distributed over the entire surface. Occasionally, small granules, coni, and verrucae of up to 1.5 µm diameter are interspaced. The spines and bacula are straight or curved and have sharp or rounded tips. Sculptural elements are sometimes absent close to the laesura.

Dimensions: Longer diameter 32 (43) 62 µm (13 specimens); shorter diameter in equatorial view 21 (25) 31 µm (8 specimens measured); shorter diameter in polar view 24 (33) 40 µm (5 specimens).

Occurrence: Sections QH/CI, CBO, CBN, CHM.

Comparisons: Clavatosporis Song and Zhong includes monolete spores with predominantly baculate ("rod-shaped") ornamentation and rough or finely granulate surface (Song and Zhong, 1984; Song et al., 1999). Only five species were found in the literature (i.e., *C. baculus*, *C. elegans* Song and Zhong, *C. elongatus* Song and Zhong, *C. gemmabaculus* Song and Zhong, and *C. laxabaculus* Song and Zhong), all from the Cenozoic of southern China (Song and Zhong, 1984; Song et al., 1999). The most similar is *C. elegans* which also has bacula with rounded and sharp tips. The wide range in the morphology of the sculptural elements distinguishes *C. varians* from *C. elegans* and the other *Clavatosporis* species.

Genus: **Microreticulatisporites** Knox 1950 emend. Potonié and Kremp 1954

Type species: Microreticulatisporites lacunosus (Ibrahim) Knox 1950

Microreticulatisporites patagonicus De Benedetti and Zamaloa sp. nov.

Plate VI, Figs. 22–26

Etymology: The epithet “patagonicus” refers to the Patagonian region.

Type locality: Cerro Buitre Norte locality, La Colonia Fm., Chubut Province, Argentina.

Holotype: MPEF-PA 929 (Plate VI, 22).

Paratypes: MPEF-PA 930 (Plate VI, 23).

Additional material: MPEF-PA 628, 828, 863, 873, 927, 928, 946, 955, 962, 989.

Stratigraphic horizon: La Colonia Formation, Maastrichtian to early Danian.

Diagnosis: Spore trilete, amb rounded triangular to subcircular. Laesurae about 3/4 spore radius or extended to the margin, with raised membranous lips. Exine 1.4–2.6 µm thick, irregularly reticulated. Lumina 0.5–2.0 µm diameter, decreasing inward; muri/ridges 0.5–3.0 µm wide. An apiculate, granulate, or verrucate element, sometimes develops at the intersections of the muri. Outline irregularly crenulated.

Description: The spores are trilete, with a subtriangular to subcircular amb, and with straight to convex sides, rarely slightly concave. The laesurae are straight to slightly undulated, extended 3/4 the spore radius or to the margin, with raised membranous lips of 0.8–1.2 µm high. The exine is 1.4–2.6 µm thick, irregularly reticulated. The sculpture is composed of low muri or ridges of 0.5–1.0 µm wide, delimiting small subcircular to polygonal lumina of 0.5–2.0 µm diameter. The reticulum is sometimes incomplete, with some specimens having patches without lumina of up to 3 µm diameter. Occasionally, the muri vary slightly in high. The diameter of the lumina decreases inward like a funnel. Sometimes, at the intersections of the muri, an apiculate, granular, or verrucate element of 0.5–1.0 µm in diameter, develops giving the spore an irregularly crenulated outline.

Dimensions: Equatorial diameter 19 (26) 34 µm (40 specimens measured).

Studied material: MPEF-PA 145, 147, 149, 168,170, 171, 652, 653, 688, 690, 692, 750, 752, 803, 827, 870, 874, 922, 929, 930.

Occurrence: Sections QH/CI, CBO, CBN, CHM.

Comparisons: The genus includes about 150 species that range in age from the Carboniferous to the Cenozoic (e.g., Palynodata Inc. and White, 2006; Frojdová et al., 2017). *M. patagonicus* possesses the typical perforations of the exine forming a negative reticulum but also has an apiculate sculpture, a feature that differentiates it from most species of the genus, such as *M. diatretus* Norris from the Lower Cretaceous of England (Norris, 1969), *M. nobilis* (Wicher) Knox from the Carboniferous of Germany and Czech Republic (Knox, 1950; Brousmiche-Delcambre et al., 1997), and *M. fundatus* Hoffmeister et al. from the Carboniferous of USA (Hoffmeister et al., 1955). *M. harrisonii* Peppers from the Carboniferous of the Czech Republic has also an apiculate sculpture but it has smaller lumina than *M. patagonicus* (Frojdová et al., 2017). *M. lacunosus* from the Carboniferous of Germany is larger (Potonié and Kremp, 1954). *M. crassiexinous* Brenner from the Lower Cretaceous of the USA is larger and has a thicker exine (Brenner, 1963). *M. densus* Dutta and Sah and *M. languidus* Dutta and Sah from the Eocene of India are slightly larger and have smaller lumina (Dutta and Sah, 1970).

4. DISCUSSION

4.1. Palynological diversity, living analogs, and paleoenvironment

Approximately 240 palynotaxa were identified in the studied assemblages of the La Colonia Fm. Spores comprise 32% of the diversity, pollen grains represent 36%, and the remaining 32% includes algal and fungal remains. Between the 76 spore taxa recorded, the relative percentages of bryophytes, lycophytes, and ferns are ~10%, ~20%, and ~%70, respectively. The number of recorded species among the sections differs notably. Almost all the spore taxa were recorded in the sections CBO and CBN (66 and 74, respectively), while approximately half were recorded in QH/CI and CHM (38 and 43, respectively). This is probably related to the

number of studied samples per section rather than to paleoecological preferences and/or paleogeographic distribution (Fig. 1; Table 1).

Bryophytes include representatives of the three major groups: hornworts, liverworts, and mosses (Table 1). Among them, the spores of *Reboulisporites* and *Zlivisporis* are related to the Ricciaceae, a family whose living representatives are adapted to aquatic life and are commonly found on the surface of eutrophic stagnant water bodies (e.g., Mahabalé, 1968; Scafati et al., 2009). Spores related to the modern genus *Sphagnum* L. that grow today in very wet areas such as peat bogs, swamp forests, or wetlands (e.g., Gunnarsson, 2005; Sundberg and Rydin, 2008) occurred along all the stratigraphic sections.

Lycophytes include members of Lycopodiaceae and Selaginellaceae (Table 1). *Camarozonosporites* species are similar to the spores produced by *Palhinhaea cernua* (L.) Vasc. and Franco (e.g., Ramos Giacosa et al., 2016) and some species of *Lycopodiella* Holub (e.g., Tryon and Lugardon, 1991). As we mentioned above, the spores of *Acylomorus silviae* and *Lusatisporis choiols* exhibit high morphological variation, and we consider that the same species of Selaginellaceae probably produced them. *Lusatisporis perinatus*, *Evansispora lacerata*, and *Perotrilites papillatus* are all first records for Argentina. *L. perinatus* is remarkably similar to the spores produced by *Selaginella fusca* Silveira (e.g., Shatilova et al., 2016). *E. lacerata* and *P. papillatus* are both similar to the spores produced by *Lycopodium volubile* G. Forst. but also to those produced by some species of *Selaginella* Willk. (Raine, 2008). Lycophytes are worldwide distributed and predominantly in the tropics, showing diversified habitats with tropical, subtropical, temperate, and xerophytic species (Tryon and Lugardon, 1991; Zhou et al., 2015).

Spores of ferns are well represented, including members of six orders, ten families, and several other species of unknown affinities (Table 1).

Cyatheales is represented by three species (*Cibotiidites auriculatus*, *C. tuberculiformis*, and *Cyatheacidites annulatus*). *C. auriculatus* has been related to the Cibotiaceae/Dicksoniaceae

568 (Archangelsky and Villar de Seoane, 1998; Vallati et al., 2020), whereas *C. tuberculiformis* is
569 related to *Dicksonia squarrosa* Foster, a tree fern endemic to New Zealand (Dettmann, 1963;
570 Lee et al., 2016). *C. annulatus* is allied with extant *Lophosoria quadripinnata* (Gmel.) C. Chr. is a
571 dominant forest floor fern living in temperate or tropical climates from Central America to
572 Patagonia (Hill et al., 2001; Lee et al., 2016).
573 Gleicheniales is represented by six species related to the three families currently recognized
574 within the order. *Cibotiumspora jurienensis* is related to *Cheiropleuria* C. Presl (Dipteridaceae),
575 distributed today in temperate and tropical Asia (Kato et al., 2001). *Clavifera triplex* and
576 *Gleicheniidites senonicus* are related to the tropical ferns *Dicranopteris* Bernh. and *Gleichenia*
577 Sm. (Gleicheniaceae) (e.g., Tryon and Lugardon, 1991). *Dictyophyllidites harrisii*,
578 *Matonisporites phlebopteroides*, and *Phlebopterisporites equiexinus* are similar to the spores of
579 *Matonia* R. Brown and *Phanerosorus* Copeland (Matoniaceae) from southeast Asia (Van
580 Konijnenburg-Van Cittert, 1993; Wang and Mei, 1999; Barbacka et al., 2016).
581 Osmundales comprises *Baculatisporites comaumensis, Osmundacidites diazii*, and
582 *Osmundacidites* sp. 1; these are similar to the spores produced by modern *Osmunda* L., *Todea*
583 Willd ex Bernh., and *Leptopteris* Presl (e.g., Tryon and Lugardon, 1991). Osmundales is
584 monotypic and includes only the family Osmundaceae, which today has a worldwide distribution
585 in temperate to tropical regions (Tryon and Lugardon, 1991).
586 Among the Polypodiales, *Tuberculatosporites parvus* has been related to the
587 Cystopteridaceae (Archangelsky, 1972), particularly with *Cystopteris* Bernh. that has
588 cosmopolitan distribution and in the Americas is found from Alaska to Tierra del Fuego (Tryon
589 and Lugardon, 1991). Polypodiaceae include *Laevigatosporites ovatus* and maybe
590 *Polypodiidites speciosus*; the latter is like the spores produced by the paleotropical ferns of the
591 genus *Microsorum* Link but also to the pan-subtropical genus *Nephrolepis* Schott of the
592 Davalliaceae (Archangelsky, 1972).

Salviniales includes the heterosporous water fern families Marsileaceae and Salviniaceae, both well represented in the La Colonia Fm. (De Benedetti et al., 2021). Thirteen spore species, including microspores and megaspores, were identified (Table 1). Marsileaceae comprises at least two paired species of megaspores/microspores that probably grew as rooted semi-aquatics (Cúneo et al., 2013; De Benedetti et al., 2021). They are *Molaspora lobata*/*Crybelosporites pannuceus*, which were found associated with macrofossils of *Regnellidium thomas-taylorii* Cúneo et al., and *Molaspora reticulata*/*Gabonisporis cristata*. Salviniaceae comprises at least three *Azolla* species (*A. andreisii*, *A. coloniensis*, and *A.* sp. cf. *A. keuja*). Only *A. coloniensis* was found intimated to macrofossils (Hermsen et al., 2019). *Azolla* sp. 1 may correspond to the microspore massulae of *A. andreisii* (De Benedetti et al., 2021). It was interpreted that the three species probably grew as free floating and fully aquatic plants as modern *Azolla* (Lumpkin and Plucknett, 1980). Heterosporous ferns are characterized not only by heterospory and monomegaspory but also by the arrangement of spores into unusual reproductive structures that do not show apparent similarities to the sporangia-bearing leaves of homosporous ferns (Bateman and DiMichele, 1994; Nagalingum et al., 2006). In modern Marsileaceae, spores are contained in elliptical to globose sclerenchymatous sporocarps, which have a thick wall that protects them against dryness and mechanical damage from herbivorous insects (Nagalingum et al., 2006). These sporocarps are long-persistent structures that display remarkably rapid establishment of new sporophytes, making them well suited to growth in intermittent and ephemeral aquatic habitats (Pryer, 1999). *Azolla* occurs in ponds, ditches, and paddy fields of warm-temperate and tropical regions throughout the world, and it has often been found growing in association with other floating aquatic weeds such as *Lemna* L., *Salvinia* Ség., *Eichhornia* Kunth, *Pistia* L., and *Spirodela* Schleid. (Lumpkin and Plucknett, 1980). The other salvinialean species (including the new species *Thecaspora polygonalis*) found in the La Colonia deposits likely grew in similar habitats (either as free-

floating or rooted macrophytes). These records indicate the presence of a low-energy freshwater environment, such as ponds, lakes, and river marshes.

Among the Schizaeales, Anemiaceae is represented by *Palaeomohria patagonica*, a species that has been previously recorded in Aptian-Coniacian deposits of Patagonia (Archangelsky, 2009; Santamarina et al., 2021; Perez Loinaze et al., 2021). The presence of this taxon in the La Colonia Fm. extends its biostratigraphic range to the Maastrichtian. Similar forms are found today in *Anemia* Sw., particularly in the subgenera *Anemiorrhiza* Prantl and *Mohria* (Sw.) Mickel (Santamarina et al., 2021). Other cicatricose spores related to the Anemiaceae/Schizaeaceae from La Colonia Fm. include *Cicatricosisporites ornatus* and *Cicatricososporites eocenicus*, constituting the first record in Argentina. *C. ornatus* was previously known from the Late Cretaceous to the Eocene of North America (e.g., Srivastava, 1972; Srivastava and Braman, 2013; Fensome et al., 2016; Kumar, 2019) and from the Tithonian–Berriasian of Sri Lanka (Weerakoon et al., 2021) whereas *C. eocenicus* was recorded from the Lower Cretaceous to the Oligocene of Europe, North and South America, Asia, and Africa (e.g., Selling, 1944; Jansonius and Hills, 1976; Kimyai, 1993; Jaramillo and Dilcher, 2001; Eisawi and Schrank, 2009; Fensome et al., 2016; Huang et al., 2021; Mander et al., 2023). Lygodiaceae is represented by *Klukisporites pseudoreticulatus*, which is similar to the pantropical spores of *Lygodium* Swartz (Van Konijnenburg-Van Cittert, 1981) and has representatives in northern Argentina (Tryon and Lugardon, 1991).

As interpreted by Cúneo et al. (2014) and later supported by palynological data published by De Benedetti et al. (2023a, 2023b), the La Colonia Fm. was part of a suite of coastal plains deposits bathed by shallow seas intercalated with barrier island/lagoon complexes that promoted the proliferation and preservation of aquatic plant communities. The La Colonia spore flora presented herein, combined with the previously described autochthonous and allochthonous elements, strongly reinforces this environmental interpretation for the La Colonia Fm.

644

645 *4.2. The K–Pg transition*

646 The K-Pg boundary has been identified mainly by the occurrence of a “boundary claystone”
647 and anomalous amounts of iridium, mostly in localities from the Northern Hemisphere (Schulte
648 et al., 2010; Jones et al., 2023). Unfortunately, records of layers of iridium are scarce in the
649 Southern Hemisphere, resulting in a poor understanding of the effect of the asteroid impact on
650 the biota of half of the planet (e.g., Schulte et al., 2010; Bercovici et al., 2012; Fastovsky and
651 Bercovici, 2016; Bercovici and Vellekoop, 2017; Bermúdez et al., 2019).

652 U-Pb geochronologic, biostratigraphic, and magnetostratigraphic data indicate that the La
653 Colonia Formation is Maastrichtian to early Danian in age; and only at the Cerro Buitre Norte
654 section was the K-Pg boundary recognized (Clyde et al., 2021). Therefore, the palynological
655 information from the La Colonia deposits represents a valuable contribution to understanding
656 the floristic changes across the K-Pg interval in southern latitudes.

657 Out of the 76 spore taxa reported here, 20 are restricted to Maastrichtian samples, while only
658 one species is restricted to Danian samples (i.e., *Cicatricosisporites ornatus*, which is a
659 singleton). Nevertheless, eight of the 20 taxa recorded in the Maastrichtian levels of the La
660 Colonia Fm. (i.e., *Aequitriradites spinulosus*, *Azolla* sp. cf. *A. keuja*, *Reboulisporites fuegiensis*,
661 *Azollopsis intermedia*, *Azollopsis tomentosa*, *Concavisporites* sp., *Phlebopterisporites*
662 *equiexinus*, and *Todisporites major*) were also found in other Paleogene deposits of Patagonia
663 and/or South America and can be excluded from those that did not cross the K-Pg boundary.
664 Additionally, some taxa are poorly recorded in the La Colonia Maastrichtian levels (i.e.,
665 *Cicatricosisporites* sp. 2, *Latrobosporites* sp. cf. *L. marginis,* and *Ghoshispora* sp.) and can also
666 be excluded from those not crossing the K-Pg boundary. Based on this, we hypothesize that
667 only nine species (i.e., *Taurocusporites segmentatus*, *Evansispora lacerata*, *Kraeuselisporites*
668 *alexii*, *Laevigatosporites* sp. 1, *Ariadnaesporites micromedusus*, *Paleoazolla patagonica*,
669 *Palaeomohria patagonica*, *Biretisporites* sp. 1, and *genus et species indet.*) are constrained to

the Maastrichtian, and that the percentage of spore species that became extinct at the La Colonia K-Pg boundary is approximately 12%.

Traditionally, the fern spike has been interpreted as the initial phase of recovery of land plants (or pioneer vegetation) from the K-Pg impact winter (Orth et al., 1981; Tschudy et al., 1984; Saito et al., 1986; Vajda and Raine, 2003). However, it is now known to have initiated within rather than above the K-Pg boundary clay in Gorgonilla Island and North America (Vajda and Bercovici, 2014; Berry, 2023). The dominant fern spore in these localities was *Cyathidites minor*, which has been primarily interpreted as produced by "tree ferns" in several localities worldwide (Vajda et al., 2001; Kroeger, 2002; Vajda and McLoughlin, 2004; Upchurch et al., 2007; Spicer and Collinson, 2014; Renne et al., 2018; Thomas and Cleal, 2022). However, Berry (2023) proposed that tree ferns could not have had ample time to reach sporing stage if they were killed back to rhizomes or other belowground reserves (i.e., by a complete shutdown of photosynthesis and subsequent impact winter) as they have exceptionally long generation times of c. 100 y, and proposed a dennstaedtiaceous affinity, which has a generation time of only 2–4 y, and better fit contemporary estimates on how long it took for the effects of Chicxulub to wind down. La Colonia paleomagnetic data indicate the presence of Chron C29R, which contains the K-Pg boundary, and the stratigraphic interval that brackets the event or its hiatus is constrained to only a few meters (Clyde et al., 2021; Fig. 1). A fern spike has not been detected, either because it is absent or because it was not sampled as there was no event layer as a reference. *Cyathidites minor* has been recorded in both Maastrichtian and Danian samples from this section and has been related to dicksoniaceous ferns (Cúneo et al., 2014; De Benedetti et al., 2023b), although affinities with other families not related to tree ferns are also possible.

In sum, no significant changes in the species diversity of bryophytes, lycophytes, and fern spores were detected among the La Colonia Maastrichtian and Danian palynofloras. Thus, as previously indicated for pollen grains (De Benedetti et al., 2023a), there is no evidence of a mass nor significant extinction across the K-Pg boundary in the studied sections, which is

consistent with other Patagonian palynological records (e.g., Barreda et al., 2012; Povilauskas, 2017). As indicated by Wilf et al. (2023), maritime and latitudinal buffering of impact-winter temperatures may be top-level variables for K-Pg extinction severity.

5. CONCLUSIONS

In this contribution, we provide a palynological study of the bryophyte, lycophyte, and fern components of the Maastrichtian-Danian deposits of the La Colonia Fm., Chubut Province, Patagonia, Argentina. Four new species, including a lycophyte, a salvinialean, and two fern spores of unknown affinities, are described. In addition, *Lusatisporis perinatus*, *Evansispora lacerata*, *Perotrilites papillatus*, *Cicatricosisporites ornatus*, *Cicatricososporites eocenicus*, and *Undulatisporites sinuosis* are recorded for the first time in Argentina.

The diverse fern palynoflora of the La Colonia Fm. provides further critical evidence on our knowledge of the diversity at the Cretaceous-Danian Patagonian paleofloras for a better understanding of the evolution of the austral vegetation during that time span and beyond. Within this geological unit, the heterosporous water ferns are one of the most diverse groups among the pteridophytes, which, added to the high diversity of bryophytes, lycophytes, and other ferns, supports the previous interpretation of a freshwater/brackish environment for the analyzed sequence.

The vegetational dynamics across the K/Pg boundary in the La Colonia Fm. supports the hypothesis that, at least locally, the effect of the mass extinction event was less significant in Patagonia than in other parts of the Earth.

Declaration of Competing Interest

The authors declare that they have no known competing financial interests or personal relationships that could have appeared to influence the work reported in this paper.

Acknowledgments

We thank P. Puerta, A. Iglesias, M. Krause, and E. Hermsen for assistance during the 2010 field work season when the bulk of the samples were collected. This work is part of FDB's Ph.D. Thesis work completed at Facultad de Ciencias Exactas y Naturales, Universidad de Buenos Aires, Argentina and it was supported by CONICET, the National Science Foundation grants DEB-0919071, DEB-0918932, DEB-1556666, DEB-1556136, EAR-1925755, and EAR-1925481 to M.A. Gandolfo and P. Wilf, and an International Association for Plant Taxonomy (IAPT) grant to F. De Benedetti.

REFERENCES

Anselmi, G., Gamba, M.T., Panza, J.L.A., 2004. Hoja Geológica 4369-IV. Los Altares. Provincia de Chubut. Servicio Geológico Minero Argentino. Instituto de Geología y Recursos Minerales, Buenos Aires, Boletín 313, 1–98.

Archangelsky, S., 1972. Esporas de la Formación Río Turbio (Eoceno) Provincia de Santa Cruz. Revista del Museo de La Plata, 6(39), 65–100.

Archangelsky, S., 1973. Palinología del Paleoceno de Chubut. I. Descripciones sistemáticas. Ameghiniana, 10(4), 339–399.

Archangelsky, S., 2009. Biogeographic implications of Albian *Mohria*-like spores (family Anemiaceae) in SW Gondwana (Patagonia). Review of Palaeobotany and Palynology, 157(3-4), 301–308.

Archangelsky, S., Villar de Seoane, L., 1998. Estudios palinológicos de la Formación Baqueró (Cretácico), Provincia de Santa Cruz, Argentina. VIII. Ameghiniana, 35(1), 7–19.

Ardolino, A., Franchi, M., 1996. Descripción Geológica de la Hoja 4366-I Telsen. Provincia del Chubut. Dirección Nacional del Servicio Geológico. Boletín 215. Buenos Aires.

746 Barbacka, M., Pacyna, G., Pieńkowski, G., Ziaja, J., 2016. New data about *Matonia braunii*
747 (Göppert) Harris from the Early Jurassic of Poland and its ecology. Geological Quarterly, 60(4),
748 857–868.
749 Bardeen, C.G., Garcia, R.R., Toon, O.B., Conley, A.J., 2017. On transient climate change at the
750 Cretaceous–Paleogene boundary due to atmospheric soot injections. Proceedings of the
751 National Academy of Sciences, USA 114(36), E7415–E7424.
752 Barreda, V.D., Cúneo, N.R., Wilf, P., Currano, E.D., Scasso, R.A., Brinkhuis, H., 2012.
753 Cretaceous/Paleogene floral turnover in Patagonia: drop in diversity, low extinction, and a
754 *Classopollis* spike. PLoS ONE, 7(12), e52455.
755 Bateman, R. M., DiMichele, W.A., 1994. Heterospory: the most iterative key innovation in the
756 evolutionary history of the plant kingdom. Biological Reviews, 69, 345–417.
757 Batten, D.J., Kovach, W.L., 1990. Catalog of Mesozoic and Tertiary megaspores. American
758 Association of Stratigraphic Palynologists Foundation, 24, 227 p.
759 Bercovici, A., Vellekoop, J., 2017. Methods in paleopalynology and palynostratigraphy: an
760 application to the K-Pg boundary. En: Terrestrial Depositional Systems. Elsevier, pp. 127–164.
761 Bercovici, A., Vajda, V., Sweet, A., 2012. Pollen and spore stratigraphy of the Cretaceous–
762 Paleogene massextinction interval in the Northern Hemisphere. Journal of Stratigraphy 36, 165–
763 178.
764 Bermúdez, H.D., Arenillas, I., Arz, J.A., Vajda, V., Renne, P.R., Gilabert, V., Rodríguez, J.V.,
765 2019. The Cretaceous/Paleogene Boundary Deposits on Gorgonilla Island. The Geology of
766 Colombia, 3, 1–19.
767 Berry, K., 2022a. Was the K/Pg boundary *Classopollis* ‘spike’ a singular event? A review of
768 global palynological records suggests otherwise, with potentially broad implications. Rocky
769 Mountain Geology, 57(1), 35–47.

Berry, K., 2022b. A *Classopollis* “spike” in the *Rugubivesiculites* Zone of the Kayan Sandstone, western Sarawak, Borneo, suggests a Danian age for these deposits. Review of Palaeobotany and Palynology, 304, 104728.

Berry, K., 2023. Can the initial phase of the K/Pg boundary fern spike be reconciled with contemporary models of the Chicxulub impact? New insights from the birthplace of the fern spike concept. Review of Palaeobotany and Palynology, 309, 104824.

Bertelsen, F., 1972. *Azolla* species from the Pleistocene of the central North Sea area. Grana, 12(3), 131–145.

Braman, D.R., 2001. Terrestrial palynomorphs of the upper Santonian–? lowest Campanian Milk River Formation, southern Alberta, Canada. Palynology, 25(1), 57–107.

Brenner, G.J., 1963. The spores and pollen of the Potomac Group of Maryland. Maryland Board Natural Resources, Department of Geology, Mines and Water Resources, Bulletin 27, 1– 215.

Brousmiche-Delcambre, C., Lugardon, B., Coquel, R., Groubet, P., 1997. Découverte dans le bassin Houiller Sarro-Lorrain du genre *Radiitheca* (organes reproducteurs de filicophytes) et ultrastructure du genre *Microreticulatisporites*. Geobios, 30(1), 3–13.

Brugger, J., Feulner, G., Petri, S., 2017. Baby, it’s cold outside: Climate model simulations of the effects of the asteroid impact at the end of the Cretaceous. Geophysical Research Letters 44, 419–427.

Clyde, W.C., Krause, J.M., De Benedetti, F., Ramezani, J., Cúneo, N.R., Gandolfo, M.A., Smith, T., 2021. New South American record of the Cretaceous–Paleogene boundary interval (La Colonia Formation, Patagonia, Argentina). Cretaceous Research, 126, 104889.

Cookson, I.C., 1953. Difference in microspore composition of some samples from a bore at Comaum, South Australia. Australian journal of botany, 1(3), 462–473.

Cúneo, N.R., Hermsen, E.J., Gandolfo, M.A., 2013. *Regnellidium* (Salviniales, Marsileaceae) macrofossils and associated spores from the Late Cretaceous of South America. International Journal of Plant Sciences, 174(3), 340–349.

796 Cúneo, N.R., Gandolfo, M.A., Zamaloa, M.C., Hermsen, E.J., 2014. Late Cretaceous Aquatic
797 Plant World in Patagonia, Argentina. PLoS ONE, 9(8), e104749.
798 Cúneo, N.R., Andruchow-Colombo, A., De Benedetti, F., Gandolfo, M.A., 2021. D.13.
799 Megafloras de las Formaciones La Colonia y Lefipán, Cretácico Superior de Chubut. In:
800 Giacosa, R.E. (Ed.). XXI Congreso Geológico Argentino. Geología y recursos naturales de la
801 provincia del Chubut. Puerto Madryn, pp. 261–272.
802 De Benedetti, F., Zamaloa, M.C., Gandolfo, M.A., Cúneo, N.R., 2018. Heterosporous ferns from
803 Patagonia: the case of *Azolla*. In: Krings, M., Harper, C.J., Cúneo, N.R., Rothwell, G.W. (Eds.),
804 Transformative Paleobotany. Academic Press, London, pp. 361–373.
805 De Benedetti, F., Zamaloa, M.C., Gandolfo, M.A., Cúneo, N.R., 2020. Reinterpretation of
806 *Paleoazolla*: a heterosporous water fern from the Late Cretaceous of Patagonia, Argentina.
807 American Journal of Botany, 107(7), 1054–1071.
808 De Benedetti, F., Zamaloa, M.C., Gandolfo, M.A., Cúneo, N.R., 2021. Water fern spores
809 (Salviniales) from the Late Cretaceous of Patagonia, Argentina. Review of Palaeobotany and
810 Palynology, 290, 104428.
811 De Benedetti, F., Zamaloa, M.C., Gandolfo, M.A., Cúneo, N.R., 2023a. Pollen from the K–Pg
812 boundary of the La Colonia Formation, Patagonia, Argentina. Review of Palaeobotany and
813 Palynology, 104933.
814 De Benedetti, F., Zamaloa, M.C., Gandolfo, M.A., 2023b. Cretaceous-Paleocene Patagonian
815 spore and pollen clumps: new findings, alternative explanations, and opened questions. The
816 Botanical Review, 1–32. https://doi.org/10.1007/s12229-023-09297-7.
817 De Jersey, N.J., 1979. Palynology of the Permian-Triassic transition in the western Bowen
818 Basin. Geological Survey of Queensland, 374, 1–39.
819 Dettmann, M.E., 1963. Upper Mesozoic microfloras from south-eastern Australia. In
820 Proceedings of the Royal Society of Victoria, 77, 1–148.

821 Dettmann, M.E., 1995. Ultrastructure and biogeography of *Balmeisporites* Cookson and
822 Dettmann, 1958. Review of Palaeobotany and Palynology, 89, 287–296.
823 Dutta, S.K., Sah, S.C.D., 1970. Palyno-stratigraphy of the Tertiary sedimentary formations of
824 Assam: 5. Stratigraphy and palynology of South Shillong Plateau. Palaeontographica Abteilung
825 B, 131(1–4), 1–72.
826 Eisawi, A., Schrank, E., 2009. Terrestrial palynology and age assessment of the Gedaref
827 Formation (eastern Sudan). Journal of African Earth Sciences, 54(1–2), 22–30.
828 Elsik, W.C., 1966. New sporomorph genera from the Upper Cretaceous of Perú. Pollen et
829 Spores, 8, 553–564.
830 Fastovsky, D.E., Bercovici, A., 2016. The Hell Creek Formation and its contribution to the
831 Cretaceous–Paleogene extinction: A short primer. Cretaceous Research, 57, 368–390.
832 Fensome, R.A., Nøhr-Hansen, H., Williams, G.L., 2016. Cretaceous and Cenozoic dinoflagellate
833 cysts and other palynomorphs from the western and eastern margins of the Labrador–Baffin
834 Seaway. Geus Bulletin, 36, 143 p.
835 Frojdová, J., Pšeniča, J., Bek, J., Martínek, K., 2017. Revision of *Dendraena pinnatilobata*
836 Nìmejc from the Pennsylvanian of the Czech Republic. Bulletin of Geosciences, 92, 1, 75–94.
837 Gallego, J., Gandolfo, M.A., Cúneo, N.R., Zamaloa, M.C., 2014. Fossil Araceae from the Late
838 Cretaceous of Patagonia, Argentina, with implications on the origin of free-floating aquatic
839 aroids. Review of Palaeobotany and Palynology, 211, 78–86.
840 Gandolfo, M.A., Cúneo, N.R., 2005. Fossil Nelumbonaceae from the La Colonia Formation
841 (Campanian-Maastrichtian, Upper Cretaceous), Chubut, Patagonia, Argentina. Review of
842 Palaeobotany and Palynology, 133(3–4), 169–178.
843 Guler, M.V., Borel, C.M., Brinkhuis, H., Navarro, E., Astini, R., 2014. Brackish to freshwater
844 dinoflagellate cyst assemblages from the La Colonia Formation (Paleocene), Northeastern
845 Patagonia, Argentina. Ameghiniana, 51(2), 141–153.

Gunnarsson, U., 2005. Global patterns of *Sphagnum* productivity. Journal of Bryology, 27(3), 269–279.

Gunther, P., Hills, L.V., 1970. Heterospory in *Ariadnaesporites*. Pollen et Spores, 12(1), 123–130.

Hermsen, E.J., Gandolfo, M.A., Cúneo, N.R., 2014. New marsileaceous fossils from the Late Cretaceous of South America and a reevaluation of *Marsileaceaephyllum*. Plant systematics and evolution, 300, 369–386.

Hermsen, E.J., Jud, N.A., De Benedetti, F., Gandolfo, M.A., 2019. *Azolla* Sporophytes and Spores from the Late Cretaceous and Paleocene of Patagonia, Argentina. International Journal of Plant Sciences, 180(7), 737–754.

Hill, R.S., Macphail, M.K., Jordan, G.J., 2001. Macrofossils associated with the fossil fern spore *Cyatheacidites annulatus* and their significance for Southern Hemisphere biogeography. Review of Palaeobotany and Palynology, 116, 195–202.

Hills, L.V., 1967. *Ariadnaesporites*, *Capulisporites* or *Caudaspora*: a discussion. Pollen et Spores, 9, 553–562.

Hoffmeister, W.S., Staplin, F.L., Malloy, R.E., 1955. Mississippian plant spores from the Hardinsburg Formation of Illinois and Kentucky. Journal of Paleontology, 29, 3, 372–399.

Huang, H., Pérez-Pinedo, D., Morley, R.J., Dupont-Nivet, G., Philip, A., Win, Z., Aung, D.W., Licht, A., 2021. At a crossroads: The late Eocene flora of central Myanmar owes its composition to plate collision and tropical climate. Review of Palaeobotany and Palynology, 291, 104441.

Jansonius, J., Hills, L.V., 1976. Genera file of fossil spores and pollen. Department of Geology, University of Calgary, Alberta, Canada.

Jaramillo, C.A., Dilcher, D.L., 2001. Middle Paleogene palynology of Central Colombia, South America: a study of pollen and spores from tropical latitudes. Palaeontographica Abteilung B, 87–259.

871 Jones, H.L., Westerhold, T., Birch, H., Hull, P., Hédi Negra, M., Röhl, U., Sepúlveda, J.,
872 Vellekoop, J., Whiteside, J.H., Alegret, L., Henehan, M., Robinson, L., van Dijk, J., Bralower, T.,
873 2023. Stratigraphy of the Cretaceous/Paleogene (K/Pg) boundary at the Global Stratotype
874 Section and Point (GSSP) in El Kef, Tunisia: New insights from the El Kef Coring Project.
875 Geological Society of America Bulletin, 135(9-10), 2451–2477.
876 Kato, M., Yatabe, Y., Sahashi, N., Murakami, N., 2001. Taxonomic studies of *Cheiropleuria*
877 (Dipteridaceae). Blumea: Biodiversity, Evolution and Biogeography of Plants, 46(3), 513–525.
878 Kimyai, A., 1993. Eocene palynomorphs from the black diamond mines regional preserve,
879 Contra Costa County, California. Palynology, 17(1), 101–113.
880 Knox, E.M., 1950. The spores of *Lycopodium*, *Phylloglossum*, *Selaginella* and *Isoetes*, and their
881 value in the study of microfossils of Paleozoic age. Transactions of the Botanical Society of
882 Edinburgh 35, 211–357.
883 Kroeger, T.J., 2002. Palynology of the Hell Creek Formation (Upper Cretaceous, Maastrichtian)
884 in northwestern South Dakota: Effects of paleoenvironment on the composition of palynomorph
885 assemblages. In: Hartman, J.H., Johnson, K.R., and Nichols, D.J., eds., The Hell Creek
886 Formation and the Cretaceous-Tertiary boundary in the northern Great Plains: An integrated
887 continental record of the end of the Cretaceous: Boulder, Colorado, Geological Society of
888 America Special Paper 361, p. 457–472.
889 Kumar, A., 2019. Pollen-spore assemblages of the Navarro Group (Maastrichtian) of Texas,
890 USA: biostratigraphical and palaeoecological significance. Journal of Palaeosciences, 68(1–2),
891 147–162.
892 Lee, D.E., Lee, W.G., Jordan, G.J., Barreda, V.D., 2016. The Cenozoic history of New Zealand
893 temperate rainforests: comparisons with southern Australia and South America. New Zealand
894 Journal of Botany, 54(2), 100–127.
895 Lumpkin, T.A., Plucknett, D.L., 1980. *Azolla*: botany, physiology, and use as a green manure.
896 Economic Botany, 34(2), 111–153.

Mahabalé, T.S., 1968. Spores and pollen grains of water plants and their dispersal. Review of Palaeobotany and Palynology, 7(4), 285–296.

Malumián, N., Náñez, C., Caramés, A., 1991. Unilocular foraminifera of reticular surface from Argentina. Micropaleontology, 37(4), 393–406.

Mander, L., Jaramillo, C., Oboh-Ikuenobe, F., 2023. Descriptive systematics of Uppe Palaeocene–Lower Eocene pollen and spores from the northern Niger Delta, south eastern Nigeria. Palynology, 47(3), 2200525.

Morgan, J.V., Bralower, T.J., Brugger, J., Wünnemann, K., 2022. The Chicxulub impact and its environmental consequences. Nature Reviews Earth & Environment, 3(5), 338–354.

Nagalingum, N.S., Schneider, H., Pryer, K.M., 2006. Comparative morphology of reproductive structures in heterosporous water ferns and a reevaluation of the sporocarp. International Journal of Plant Sciences, 167(4), 805–815.

Náñez, C., Malumián, N., 2008. Paleobiogeografía y paleogeografía del Maastrichtiense marino de la Patagonia, Tierra del Fuego y la Plataforma Continental Argentina, según sus foraminíferos bentónicos. Revista Española de Paleontología, 23(2), 273–300.

Nichols, D.J., Johnson, K.R., 2008. Plants and the K-T Boundary. Cambridge University Press.

Norris, G., 1969. Miospores from the Purbeck Beds and marine Upper Jurassic of southern England. Palaeontology, 12, 574–620.

O'Gorman, J.P., 2021. The most complete specimen of *Kawanectes lafquenianum* (Sauropterygia, Plesiosauria): new data on basicranial anatomy and possible sexual dimorphism in elasmosaurids. Cretaceous Research, 125, 104836.

Oriozabala, C., Sterli, J., de la Fuente, M.S., 2020. New species of the long-necked chelid *Yaminuechelys* from the Upper Cretaceous (Campanian–Maastrichtian) of Chubut, Argentina. Cretaceous Research, 106, 104197.

921 Orth, C.J., Gilmore, J.S., Knight, J.D., Pillmore, C.L., Tschudy, R.H., Fassett, J.E., 1981. An
922 iridium abundance anomaly at the palynological Cretaceous-Tertiary boundary in northern New
923 Mexico. Science, 214(4527), 1341–1343.
924 Paden Phillips, P., Félix, C.J., 1971. A study of lower and middle Cretaceous spores and pollen
925 from the southwestern United States. I. Spores. Pollen et Spores, 13(2), 279–348.
926 Page, R., Ardolino, A., de Barrio, R.E., Franchi, M., Lizuain, A., Page, S., Silva Nieto, D., 1999.
927 Estratigrafía del Jurásico y Cretácico del Macizo de Somún Curá, provincias de Río Negro y
928 Chubut. In: Caminos R. (Ed.), Geología Regional Argentina, Servicio Geológico Minero
929 Argentino. Instituto de Geología y Recursos Minerales, Buenos Aires. Anales 29, pp. 460–488.
930 Palynodata Inc., White, J.M., 2006. Palynodata Datafile: 2006 version, with Introduction by J.M.
931 White. Geological Survey of Canada Open File 5793, 1 CD-ROM.
932 Panzeri, K.M., Cavalli, S.G., Muñoz, N.A., Cione, A.L., 2020. *Metaceratodus baibianorum*, a
933 new dipnoan species from the Upper Cretaceous of southern South America supported by
934 traditional and geometric morphometric analyses. Journal of Vertebrate Paleontology, 40(2),
935 e1769640.
936 Papú, O.H., 2002. Nueva microflora de edad maastrichtiana en la localidad de Calmu-Co, sur
937 de Mendoza, Argentina. Ameghiniana, 39, 415–426.
938 Perez Loinaze, V.P., Giordano, S.R., Limarino, C.O., 2021. Late Cretaceous palynomorphs from
939 the Golfo San Jorge Basin, Argentina. Journal of South American Earth Sciences, 107, 103151.
940 Perez Loinaze, V.S., Vera, E.I., Moyano-Paz, D., Coronel, M.D., Manabe, M., Tsuihiji, T.,
941 Novas, F.E., 2023. Maastrichtian palynological assemblages from the Chorrillo Formation,
942 Patagonia, Argentina. Review of Palaeobotany and Palynology, 314, 104893.
943 Potonié, R., Kremp, G., 1954. Die Gattungen der palaozoischen Sporae dispersae undihre
944 Stratigraphie. Geologisches Jahrbuch, 69, 111–194.
945 Povilauskas, L., 2017. Palynostratigraphy of the Cretaceous–Paleogene in the Austral Basin,
946 SW Santa Cruz Province, Argentina. Revista Brasileira de Paleontologia, 20, 299–320.

947 Pryer, K.M., 1999. Phylogeny of marsileaceous ferns and relationships of the fossil *Hydropteris*
948 *pinnata* reconsidered. International Journal of Plant Sciences, 160(5), 931–954.
949 Raine, J.I., 2008. Zonate lycophyte spores from New Zealand Cretaceous to Paleogene
950 strata. Alcheringa, 32(2), 99–127.
951 Ramos Giacosa, J., Morbelli, M.A., Giudice, G.E., Gorrer, D.A., 2016. Spore morphology and
952 wall ultrastructure of Lycopodiaceae from northwest Argentina. Review of Palaeobotany and
953 Palynology, 225, 84–94.
954 Raup, D.M., Sepkoski Jr, J.J., 1982. Mass extinctions in the marine fossil record. Science,
955 215(4539), 1501–1503.
956 Renne, P.R., Arenillas, I., Arz, J.A., Vajda, V., Gilabert, V., Bermúdez, H.D., 2018. Multi-proxy
957 record of the Chicxulub impact at the Cretaceous-Paleogene boundary from Gorgonilla Island,
958 Colombia. Geology, 46(6), 547–550.
959 Sacomani, L.E., Panza, J.L.A., Parisi, C., Pezzuchi, H.D., Ardolino, A.A., 2007. Hoja Geológica
960 4366-III. Las Plumas. Servicio Geológico Minero Argentino. Instituto de Geología y Recursos
961 Minerales. Buenos Aires. Boletín 291, 74 p.
962 Saito, T., Yamanoi, T., Kaiho, K., 1986. End-Cretaceous devastation of terrestrial flora in the
963 boreal Far East. Nature, 323(6085), 253–255.
964 Santamarina, P.E., Barreda, V.D., Iglesias, A., Varela, A.N., 2021. *Palaeomohria* Spores from
965 the Cenomanian in Patagonia, Argentina. Ameghiniana, 58(3), 289–296.
966 Saxena, R.K., Tripathi, S.K.M., 2012. Seven decades of Indian Tertiary spore-pollen floras: A
967 Compendium. AASP Contribution Series, 45, 1–182.
968 Scafati, L., Melendi, D.L., Volkheimer, W., 2009. A Danian subtropical lacustrine palynobiota
969 from South America (Bororó Formation, San Jorge Basin, Patagonia-Argentina). Geologica
970 Acta: an international earth science journal, 7(1), 35–62.
971 Schulte, P., Alegret, L., Arenillas, I., Arz, J.A., Barton, P.J., Bown, P.R., Bralower, T.J.,
972 Christeson, G.L., Claeys, P., Cockell, C.S., Collins, G.S., Deutsch, A., Goldin, T.J., Goto, K.,

973 Grajales-Nishimura, J.M., Grieve, R.A.F., Gulick, S.P.S., Johnson, K.R., Kiessling, W., Koeberl,
974 C., Kring, D.A., MacLeod, K.G., Matsui, T., Melosh, J., Montanari, A., Morgan, J.V., Neal, C.R.,
975 Nichols, D.J., Norris, R.D., Pierazzo, E., Ravizza, G., Rebolledo-Vieyra, M., Reimold, W.U.,
976 Robin, E., Salge, T., Speijer, R.P., Sweet, A.R., Urrutia-Fucugauchi, J., Vajda, V., Whalen, M.T.,
977 Willumsen, P.S., 2010. The Chicxulub asteroid impact and mass extinction at the Cretaceous-
978 Paleogene boundary. Science, 327(5970), 1214–1218.
979 Selling, O.H., 1944. A new species of *Schizaea* from Melanesia, and some connected problems.
980 Svensk Botanisk Tidskrift Bd, Stockholm, 38(3), 207–225.
981 Shatilova, I., Rukhadze, L., Kokolashvili, I., 2016. Representatives of the family
982 Hamamelidaceae in Neogene of Georgia. Tbilisi: Georgian National Museum, 80 pp.
983 Singh, C., 1983. Cenomanian microfloras of the Peace River area, northwestern Alberta.
984 Alberta Research Council, Bulletin 44, 332 p.
985 Song, Z., Zhong, B., 1984. Tertiary sporo-pollen assemblages from Jinggu, Yunnan. Bull.
986 Nanjing Inst. Geol. Palaeontol. Acad. Sin., 8, 1–53.
987 Song, Z., Li, M., Wang, W., Zhao, C., Zhu, Z., Zheng, Y., Zhang, Y., Wang, D., Zhou, S., Zhao,
988 Y., 1999. Fossil spores and pollen from China. Volume 1: The Late Cretaceous and Tertiary
989 Spores and Pollen. Science Press, Beijing, China, 910 p.
990 Spicer, R.A., Collinson, M.E., 2014. Plants and floral change at the Cretaceous-Paleogene
991 boundary: Three decades on. Special Paper of the Geological Society of America, 505, 117–
992 132.
993 Srivastava, S.K., 1972. Systematic description of some spores from the Edmonton Formation
994 (Maestrichtian), Alberta, Canada. Palaeontographica B 139, 1–46.
995 Srivastava, S.K., Braman, D.R., 2013. The palynostratigraphy of the Edmonton Group (Upper
996 Cretaceous) of Alberta, Canada. Palynology 37, 1–27.
997 Stiles, E., Wilf, P., Iglesias, A., Gandolfo, M.A., Cúneo, N.R., 2020. Cretaceous–Paleogene
998 plant extinction and recovery in Patagonia. Paleobiology, 46(4), 445–469.

Strasburger, E., 1873. Ueber *Azolla*. Jena, Hermann Dabis.

Sundberg, S., Rydin, H., 2002. Habitat requirements for establishment of *Sphagnum* from spores. Journal of Ecology, 90(2), 268–278.

Sweet, A.R., Hills, L.V., 1974. A detailed study of the genus *Azollopsis*. Canadian Journal of Botany 52, 1625–1642.

Thomas, B.A., Cleal, C.J., 2022. Pteridophytes as primary colonisers after catastrophic events through geological time and in recent history. Palaeobiodiversity and Palaeoenvironments, 102(1), 59–71.

Thompson, J.B., Ramírez-Barahona, S., 2023. No phylogenetic evidence for angiosperm mass extinction at the Cretaceous–Palaeogene (K-Pg) boundary. Biology Letters, 19(9), 20230314.

Traverse, A., 2007. Paleopalynology. 2nd ed. Springer Science & Business Media, Pennsylvania, 813 pp.

Tryon, A.F., Lugardon, B., 1991. Spores of the Pteridophyta: surface, wall structure, and diversity based on electron microscope studies. Springer-Verlag, New York Inc., 648 pp.

Tschudy, R.H., 1966. Associated megaspores and microspores of the Cretaceous genus *Ariadnaesporites* Potonié, 1956, emend. United States Geological Survey, Professional Paper 550, D76–D82.

Tschudy, R.H., Pillmore, C.L., Orth, C.J., Gilmore, J.S., Knight, J.D., 1984. Disruption of the terrestrial plant ecosystem at the Cretaceous-Tertiary boundary, Western Interior. Science, 225(4666), 1030–1032.

Upchurch, G.R., Lomax, B.H., Beerling, D.J., 2007. Paleobotanical evidence for climatic change across the Cretaceous-Tertiary boundary, North America: Twenty years after Wolfe and Upchurch. Courier-Forschungs Institut Senckenberg, 258, 57–74.

Vajda, V., Raine, J.I., 2003. Terrestrial palynology of the Cretaceous/Tertiary boundary at mid-Waipara River, North Canterbury, New Zealand. New Zealand Journal of Geology and Geophysics, 46, 255–273.

1025 Vajda, V., McLoughlin, S., 2004. Fungal proliferation at the Cretaceous-Tertiary boundary.
1026 Science, 303(5663), 1489–1489.
1027 Vajda, V., Bercovici, A., 2014. The global vegetation pattern across the Cretaceous–Paleogene
1028 mass extinction interval: A template for other extinction events. Global and Planetary
1029 Change, 122, 29–49.
1030 Vajda, V., Raine, J.I., Hollis, C.J., 2001. Indication of global deforestation at the Cretaceous-
1031 Tertiary boundary by New Zealand fern spike. Science, 294, 1700–1702.
1032 Vajda, V., Raine, J.I., Hollis, C.J., Strong, C.P., 2004. Global effects of the Chicxulub impact on
1033 terrestrial vegetation—review of the palynological record from New Zealand Cretaceous/Tertiary
1034 boundary. Cratering in Marine Environments and on Ice, 57–74.
1035 Vallati, P., De Sosa Tomas, A., Casal, G., Calo, M., 2017. Salviniales from the Late Cretaceous
1036 of the Golfo San Jorge Basin. Cretaceous Research, 74, 45–55.
1037 Vallati, P., Tomas, A.D.S., Casal, G., 2020. A Maastrichtian terrestrial palaeoenvironment
1038 close to the K/Pg boundary in the Golfo San Jorge basin, Patagonia, Argentina. Journal
1039 of South American Earth Sciences, 97, 102401.
1040 Van Konijnenburg-Van Cittert, J.H., 1981. Schizaeaceous spores in situ from the Jurassic of
1041 Yorkshire, England. Review of Palaeobotany and Palynology, 33(2-4), 169–181.
1042 Van Konijnenburg-Van Cittert, J.H., 1993. A review of the Matoniaceae based on in situ spores.
1043 Review of Palaeobotany and Palynology, 78(3-4), 235–267.
1044 Wang, Y., Mei, S., 1999. Fertile organs and in situ spores of a matoniaceous fern from the
1045 Lower Jurassic of West Hubei. Chinese Science Bulletin, 44(14), 1333–1337.
1046 Weerakoon, W.A.P., Joshi, H., Aggarwal, N., Jha, N., Jayasena, H.A.H., Yakandawala, D.,
1047 Chandrajith, R., Ratnayake, N.P., Tiwari, P., 2021. Late Jurassic-Early Cretaceous
1048 palynostratigraphy and palaeoclimate in the Andigama Basin, Sri Lanka. Journal of Asian Earth
1049 Sciences: X, 6, 100067.

Wilf, P., Carvalho, M.R., Stiles, E., 2023. The end-Cretaceous plant extinction: heterogeneity, ecosystem transformation, and insights for the future. Cambridge Prisms: Extinction, 1, e14, 1–10.

Yi, S., Batten, D.J., 2002. Palynology of Upper Cretaceous (uppermost Campanian–Maastrichtian) deposits in the South Yellow Sea Basin, offshore Korea. Cretaceous Research 23, 687–706.

Zhou, X.M., Jiang, L.J., Zhang, L., Gao, X.F., He, Z.R., Zhang, L.B., 2015. Spore morphology of *Selaginella* (Selaginellaceae) from China and its systematic significance. Phytotaxa, 237(1), 001–067.

Figure 1. 1. Map showing the studied area where the La Colonia Formation outcrops, in the vicinity of the Mirasol Chico Creek, Chubut Province, Patagonia, Argentina. 2. Simplified stratigraphic sections: from left to right Quebrada del Helecho/Cañadón del Irupé (QH/CI), Cerro Bosta (CBO), Cerro Buitre Norte (CBN), and Chiva Muerta (CHM). QH/CI and CBO were modified from Cúneo et al. (2014). The CBN is a composite stratigraphic section (sections A and B of Fig. 2 in Clyde et al., 2021); the grey sidebar to the left indicates the magnetozone of reversed polarity that is interpreted to correlate to Chron C29R (see Clyde et al., 2021).

Table 1. Bryophyte, lycophyte, and fern spores recovered from the La Colonia Formation.

Plate I. 1–3. *Foraminisporis dailyi* (Cookson and Dettmann) Dettmann 1963. 1. MPEF-PA 580 (102.4/44.8). 2. MPEF-PA 149. 3. MPEF-PA 150. 4. *Reboulisporites fuegiensis* Zamaloa and Romero 1990. MPEF-PA 625 (101.7/41.6). 5. *Zlivisporis asper* (Srivastava) comb. nov. MPEF-PA 800 (95/32.2). 6–9. *Zlivisporis reticulatus* (Pocock) Pacltová and Simoncsics 1970. 6. MPEF-PA 622 (103.9/30.6). 7. MPEF-PA 929 (101.5/34.1). 8. MPEF-PA 150. 9. MPEF-PA 149. 10. *Aequitriradites spinulosus* (Cookson and Dettmann) Cookson and Dettmann 1961. MPEF-PA

753 (103.7/31.2). 11, 12. *Cingutriletes australis* (Cookson) Archangelsky 1972. 11. MPEF-PA 874. 12. MPEF-PA 170. 13, 14. *Tripunctisporis maastrichtiensis* (Krutzsch) Herngreen et al. 1986. 13. MPEF-PA 874. 14. MPEF-PA 171. 15. *Taurocusporites segmentatus* Stover 1962. MPEF-PA 819 (98.1/26.7). 16–18. *Camarozonosporites ambigens* (Fradkina) Playford 1971. 16. MPEF-PA 820 (98/35.1). 17. MPEF-PA 167. 18. MPEF-PA 171. 19, 20. *Camarozonosporites amplus* (Stanley) Dettmann and Playford 1968. 19. MPEF-PA 992 (93/28.2). 20. MPEF-PA 173. 21, 22. *Camarozonosporites* sp. 1. 21. MPEF-PA 803 (96.3/30.2). 22. MPEF-PA 168. 23, 24. *Latrobosporites* sp. cf. *L. marginis* Mildenhall and Pocknall 1989. 23. MPEF-PA 826 (96.5/37.5). 24. MPEF-PA 170. 25, 26. *Retitriletes eminulus* (Dettmann) Srivastava 1975. 25. MPEF-PA 752 (99.1/43.2). 26. MPEF-PA 168. 27, 28. *Sestrosporites pseudoalveolatus* (Couper) Dettmann 1963. 27. MPEF-PA 936 (107.7/29.3). 28. MPEF-PA 145. 29, 30. *Acylomorus silviae* Perez Loinaze et al. 2023. 29. MPEF-PA 926 (92.2/37.5). 30. MPEF-PA 942 (100.8/34.8).

Scale bars: 1–30 = 10 μm.

Plate II. 1–8. *Acylomorus silviae* Perez Loinaze et al. 2023. 3–5. Tetrads with *Acylomorus silviae* (A) and an anomalous form (= *Lusatisporis choiols* Perez Loinaze et al. 2023 (L)). 6, 7. Tetrad of *Acylomorus silviae*. 7. Detail of sculpture. 8. Anomalous specimen of *A. silviae* (= *L. choiols*). 1. MPEF-PA 171. 2. MPEF-PA 151. 3. MPEF-PA 926 (112.8/38). 4. MPEF-PA 928 (101.9/23.9). 5. MPEF-PA 752 (98.1/24.7). 6, 7. MPEF-PA 168. 8. MPEF-PA 750 (92.3/37.7). 9. *Lusatisporis perinatus* Krutzsch 1963. MPEF-PA 750 (92.3/37.7). 10, 11. *Ceratosporites equalis* Cookson and Dettmann 1958. 10. MPEF-PA 873 (96/20). 11. MPEF-PA 168. 12. *Densoisporites velatus* Weyland and Krieger emend. Krasnova 1961. MPEF-PA 688 (101.6/38.7). 13. *Evansispora lacerata* (Norris) Raine 2008. MPEF-PA 653 (107.5/36.3). 14, 15. *Herkosporites elliottii* Stover 1973. 14. MPEF-PA 925 (104/42.8). 15. MPEF-PA 170. 16. *Kraeuselisporites alexii* Raine 2008. MPEF-PA 958 (93.5/30.9). 17–23. *Neoraistrickia loconiensis* sp. nov. 17.

Holotype. MPEF-PA 923 (106.4/23.6). 18. MPEF-PA 924 (110.4/31.4). 19. MPEF-PA 928 (110.8/26.6). 20, 23. MPEF-PA 170. 21. MPEF-PA 150. 22. MPEF-PA 145. 24, 25. *Perotrilites papillatus* (Harris) Raine 2008. 24, 25. MPEF-PA 841 (103.2/35.7). 26, 27. *Cibotiidites auriculatus* Archangelsky and Villar de Seoane 1998. 26. MPEF-PA 656 (94.3/34.6). 27. MPEF-PA 147. 28, 29. *Cibotiidites tuberculiformis* (Cookson) Skarby 1974. 28. MPEF-PA 753 (100.8/33.7). 29. MPEF-PA 171. 30. *Cyatheacidites annulatus* Cookson ex Potonié 1956. MPEF-PA 820 (104.3/28.2).

Scale bars: 1–6, 8–22, 24–30 = 10 μm; 7 = 3 μm; 23 = 2 μm.

Plate III. 1. *Cyatheacidites annulatus* Cookson ex Potonié 1956. MPEF-PA 169. 2. *Cibotiumspora jurienensis* (Balme) Filatoff 1975. MPEF-PA 928 (101.9/41). 3, 4. *Clavifera triplex* (Bolkhovitina) Bolkhovitina 1966. 3. MPEF-PA 583 (93.9/42.6). 4. MPEF-PA 168. 5, 6. *Gleicheniidites senonicus* Ross emend. Skarby 1964. 5. MPEF-PA 873 (103.2/31.2). 6. MPEF-PA 168. 7, 8. *Dictyophyllidites harrisii* Couper 1958. 7. MPEF-PA 612 (94.6/39.5). 8. MPEF-PA 171. 9. *Matonisporites phlebopteroides* Couper 1958. MPEF-PA 922 (104.9/23.2). 10. *Phlebopterisporites equiexinus* (Couper) Juhász 1979. MPEF-PA 752 (105.5/35.8). 11, 12. *Baculatisporites comaumensis* (Cookson) Potonié 1956. 11. MPEF-PA 872 (111.1/37.4). 12. MPEF-PA 169. 13, 14. *Osmundacidites diazii* Volkheimer 1972. 13. MPEF-PA 631 (112/28.6). 14. MPEF-PA 145. 15, 16. *Osmundacidites* sp. 1. 15. MPEF-PA 630 (103.3/27). 16. MPEF-PA 168. 17. *Tuberculatosporites parvus* Archangelsky 1972. MPEF-PA 930 (110.7/38.3). 18, 19. *Laevigatosporites ovatus* Wilson y Webster 1946. 18. MPEF-PA 689 (92.8/49.5). 19. MPEF-PA 150. 20. *Laevigatosporites* sp. 1. MPEF-PA 688 (108.6/45.5). 21. *Polypodiidites speciosus* (Harris) Archangelsky 1972. MPEF-PA 948 (93.4/43.7). 22, 23. *Molaspora lobata* (Dijkstra) Hall, in Hall and Peake 1968 / *Crybelosporites pannuceus* (Brenner) Srivastava 1977. 22. Megaspore with two attached microspores (arrowheads). 23. Detail of a microspore. 22, 23. MPEF-PA 176.

24–30. *Molaspora reticulata* Campbell and Untergasser 1972 / *Gabonisporis cristata* (Stanley) Sweet 1986. 24–27. Megaspores with attached microspores. Arrowheads indicates the details of the microspores in 28, 29, and 30, respectively. 27. Megaspore with numerous microspores attached, probably the remain of a broken sporocarp. 24, 28. MPEF-PA 156. 25, 29. MPEF-PA 179. 26, 27, 30. MPEF-PA 183.

Scale bars: 1–21, 23, 28–30 = 10 μm; 22, 24–27 = 100 μm.

Plate IV. 1–18. *Azolla andreisii* De Benedetti and Zamaloa 2021. 1–6. Megaspore apparatuses. Note the variation in float arrangement and size. 7, 8. Longitudinal sections of two megaspore apparatuses. 9, 10. Details of 7 and 8, respectively. Note the perinal excrescences (arrowheads). 11. Detail of 3. Slightly broken specimen showing the excrescences of the megaspore. 12. Broken specimen showing the megaspore with excrescences. 13. Detail of an excrescence in 12. Note the absence of papillate elements towards its tip (arrowhead). 14. Detail of 5. Float with a rough surface. 15. Detail of 2. Float with granulate/papillate surface. 16. Detail of 3. Inner surface of a float. Note the perinal extensions that narrow distally to form long perinal hairs (arrowheads). 17, 18. Details of 1. Long perinal hairs with circinate/coiled tips (arrowheads) emerging between the floats. 1, 17, 18. MPEF-PA 154. 2, 3, 5, 6, 11, 14–16. MPEF-PA 181. 4. MPEF-PA 179. 7–10. MPEF-PA 185. 12, 13. MPEF-PA 183. Abbreviations: e, exine; f, float apparatus; h, perinal hairs; m, megaspore; n, endoperine; p, exoperine. 19–26. *Azolla coloniensis* De Benedetti and Zamaloa emend. Hermsen et al. 2019. 19–22. Megaspore apparatuses. Note the variation in the development of excrescences in the megaspore. 23. Detail of 22. 24. Megaspore apparatus with the floats removed. Note the central tripartite columella. 25. Detail of 19. Microspore massulae attached to the megaspore apparatus. 26. Microspores. 19, 22, 23, 25. MPEF-PA 155. 21. MPEF-PA 157. 26. MPEF-PA 156. 20. MPEF-PA 184. 24. MPEF-PA 175. 27–30. *Azolla* sp. cf. *A. keuja* Jud, De Benedetti, Gandolfo and

Hermsen 2019. 27–30. Megaspore apparatuses. Note the morphological variation of the excrescences and collar. 30. Specimen without indusium, and with at least six floats arranged in one tier. 27. MPEF-PA 184. 28. MPEF-PA 177. 29. MPEF-PA 182. 30. MPEF-PA 178. Abbreviations: co, collar; cl, columella; e, exine; f, float apparatus; g, glochidia; h, perinal hairs; i, indusium; m, megaspore; n, endoperine; p, exoperine.

Scale bars: 1–8, 12, 19–22, 24 = 100 μm; 9, 10, 13, 17, 18, 23, 25, 26 = 10 μm; 11 = 50 μm; 14–16 = 20 μm.

Plate V. 1–10. *Azolla* sp. cf. *A. keuja* Jud, De Benedetti, Gandolfo and Hermsen 2019. 1, 2. Megaspore wall. Note the columellate layer of the exoperine (arrowhead in 2). 3–5. Megaspore sculpture (3 and 5 details of Plate IV, 28). 6. Float surface (detail of Plate IV, 27). 7, 8. Megaspore apparatus with the floats removed. Note the central tripartite columella. 9. Detail of 8. Note the numerous vacuolated floats. 10. Sculpture of the columella. Note the basal attachment of the perinal hairs (arrowheads). 3, 5. MPEF-PA 177. 4. MPEF-PA 182. 1. MPEF-PA 178. 2. MPEF-PA 175. 6. MPEF-PA 184. 7. MPEF-PA 176. 8–10. MPEF-PA 185. 11. *Ariadnaesporites micromedusus* Stough 1968. MPEF-PA 977 (107.6/41.3). 12–14. *Azollopsis intermedia* Sweet and Hills 1974. 12. Microsporangiate sori. Note the individual microsporangia (mi). 13, 14. Detail of microspores. Note the elevated lips (l) and the exine walls (arrowheads). 12, 13. MPEF-PA 181. 14. MPEF-PA 157. 15, 16. *Azollopsis tomentosa* Hall 1968. 7. Megaspore apparatus with two attached microspore massulae. 8. Detail of massulae and glochidia. Note the perinal hairs arising from one of the floats of the megaspore (arrowheads). 15, 16. MPEF-PA 155. 17–23. *Thecaspora polygonalis* sp. nov. 17, 18. Holotype. MPEF-PA 767 (101.9/23.5). 22. Microsporangium remain. 23. Detail of the closely appressed specimens in another microsporangium. Note the trilete mark in 18, 20 and 23 (arrowheads). 19–21. MPEF-PA 766. 19, 20. (109.4/26.3). 21. (109.3/26.2). 22, 23. MPEF-PA 767. 22. (100.9/20.4). 23.

(113.5/22.5). 24, 25. *Genus et species indet.* Note the rhombic and scythe-shaped glochidia (arrowheads). 24. MPEF-PA 766 (113/27.8). 25. MPEF-PA 767 (101.9/23.3). 26. *Palaeomohria patagonica* Archangelsky 2009. MPEF-PA 795 (95.2/37.1). 27. *Cicatricosisporites ornatus* Srivastava 1972. MPEF-PA 949 (111.7/37.7). 28. *Cicatricosisporites* sp. 1. MPEF-PA 933 (113/43.2). 29. *Cicatricosisporites* sp. 2. MPEF-PA 612 (108.7/51.5). 30. *Cicatricososporites eocenicus* (Selling) Jansonius and Hills 1976. MPEF-PA 928 (109.2/36.4). Abbreviations: a, acrolamella; cl, columella; e, exine; f, float; h, perinal hairs; l, lips; mi, microsporangia; n, endoperine; p, exoperine; v, vacuolated structure of the floats.

Scale bars: 1, 3, 4, 6, 10, 11, 13, 14, 16–21, 23–30 = 10 μm; 2 = 5 μm; 5 = 2 μm; 7, 8, 12, 15 = 100 μm; 9 = 30 μm; 22 = 20 μm.

Plate VI. 1, 2. *Klukisporites pseudoreticulatus* Couper 1958. 1. MPEF-PA 804. (101.3/33). 2. MPEF-PA 147. 3, 4. *Biretisporites crassilabratus* Archangelsky 1972. 3. MPEF-PA 936 (98/40.2). 4. MPEF-PA 165. 5, 6. *Biretisporites* sp. 1. 5, 6. MPEF-PA 651 (96.9/47). 7, 8. *Biretisporites* sp. 2. 7. MPEF-PA 628 (110.5/39.1). 8. MPEF-PA 150. 9–12. *Clavatosporis varians* sp. nov. 9. Holotype. MPEF-PA 828 (98.7/30.6). 10. MPEF-PA 927 (109.5/27.3). 11. MPEF-PA 873 (108/19.8). 12. MPEF-PA 628 (96.1/29.7). 13. *Concavisporites* sp. cf. *C.* sp. 2 of Archangelsky 1972. MPEF-PA 870 (100.8/31). 14. *Concavissimisporites verrucosus* Delcourt and Sprumont emend. McKellar 1998. MPEF-PA 688 (112.4/42.7). 15. *Cyathidites australis* Couper 1953. MPEF-PA 452 (95.2/48.4). 16. *Cyathidites concavus* (Bolkhovitina) Dettmann 1963. MPEF-PA 870 (111.3/31.6). 17. *Cyathidites minor* Couper 1953. MPEF-PA 689 (94.6/39.9). 18. *Cyathidites patagonicus* Archangelsky 1972. MPEF- PA 978 (101.4/19.7). 19. *Deltoidospora* sp. MPEF-PA 930 (108.5/33). 20. *Granulatisporites* sp. MPEF-PA 926 (100.1/37.1). 21. *Leiotriletes regularis* (Pflug) Krutzsch 1959. MPEF-PA 614 (92.5/43.2). 22–26. *Microreticulatisporites patagonicus* sp. nov. 22. Holotype. MPEF-PA 929 (103.1/41.9). 23.

MPEF-PA 930 (111.4/30.6). 24. MPEF-PA 171. 25. MPEF-PA 145. 26. MPEF-PA 168. 27. *Peromonolites vellosus* Partridge 1973. MPEF-PA 874 (112.2/44.3). 28. *Rugulatisporites* sp. MPEF-PA 608 (93.6/36.9). 29. *Todisporites major* Couper 1958. MPEF-PA 628 (96.4/36.3). 30. *Undulatisporites sinuosis* Groot and Groot 1962. MPEF-PA 930 (112.2/34.2).

Scale bars: 1–17, 19–30 = 10 μm; 18 = 20 μm.

Figure

Click here to access/download;Figure;FIGURE 1.tif

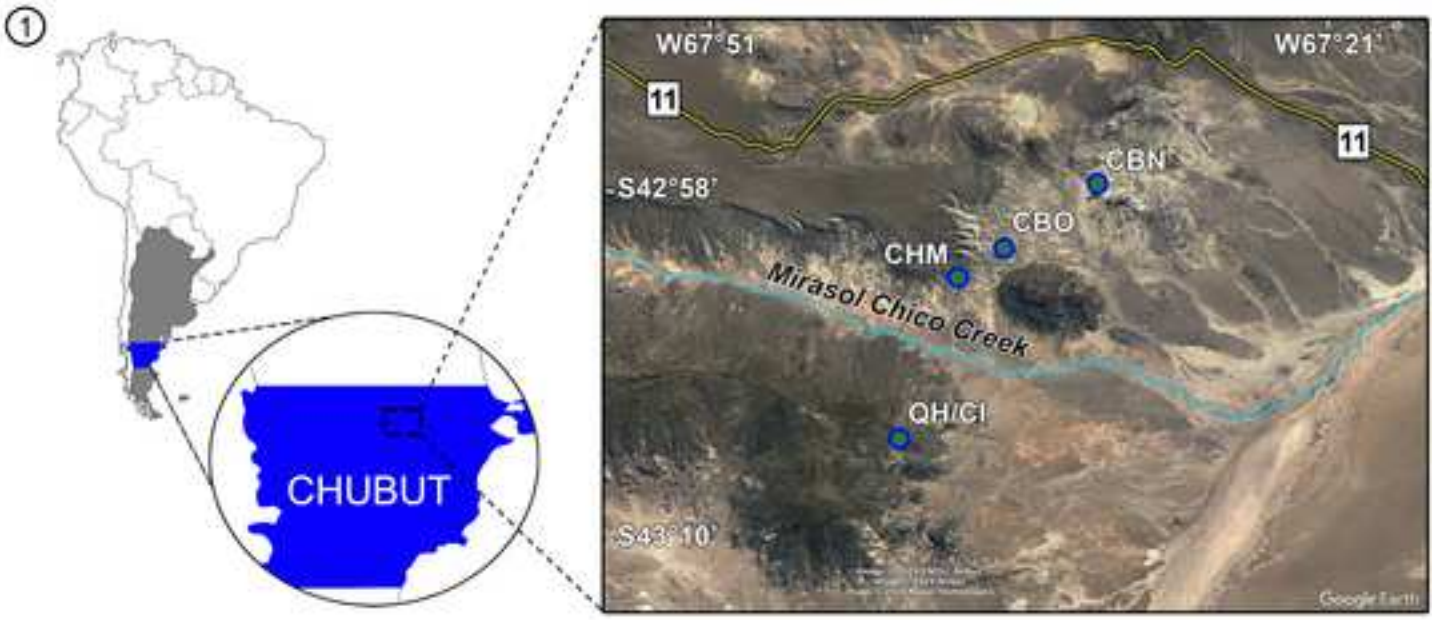

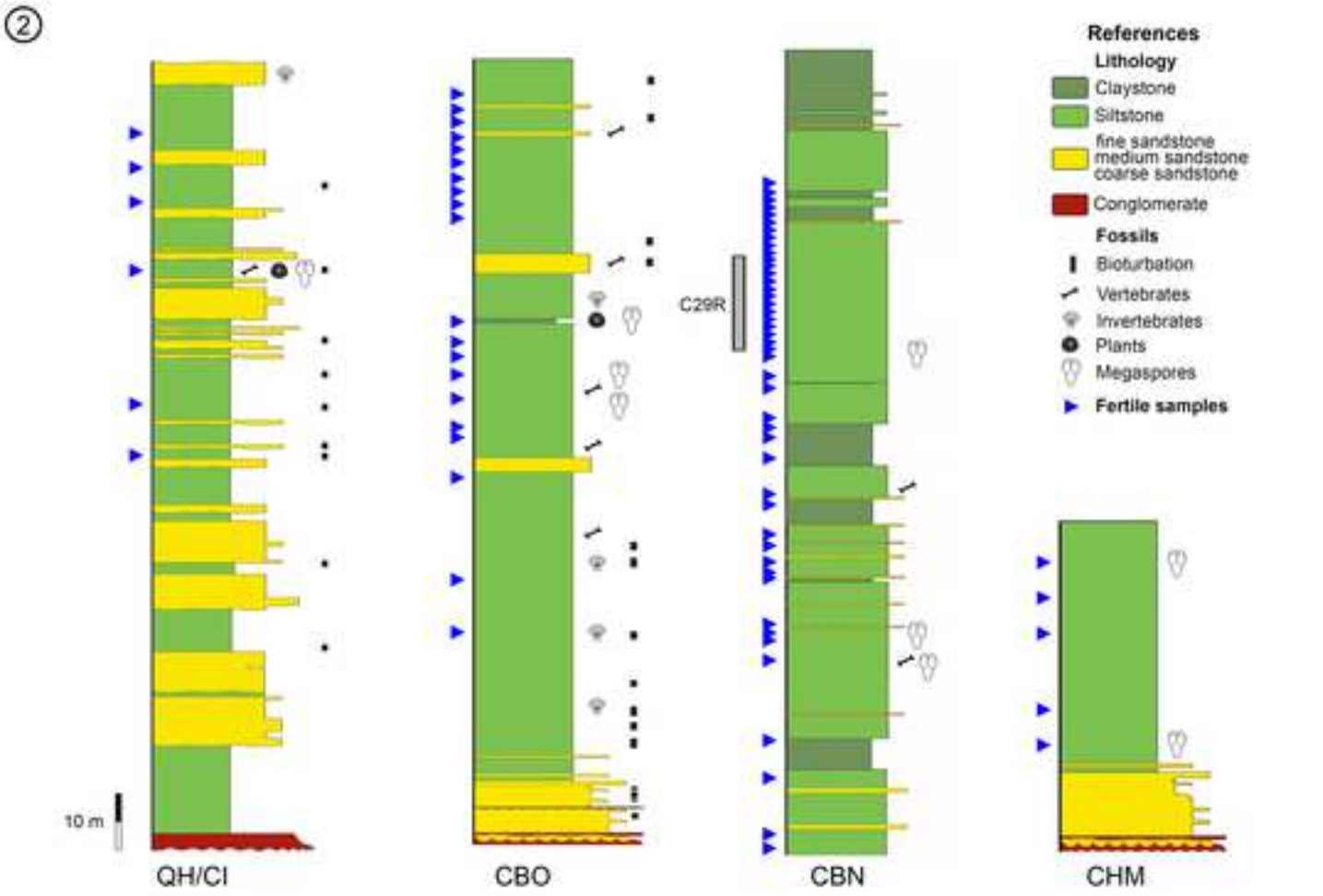

Plate I

Click here to access/download;Figure;Plate I.tif

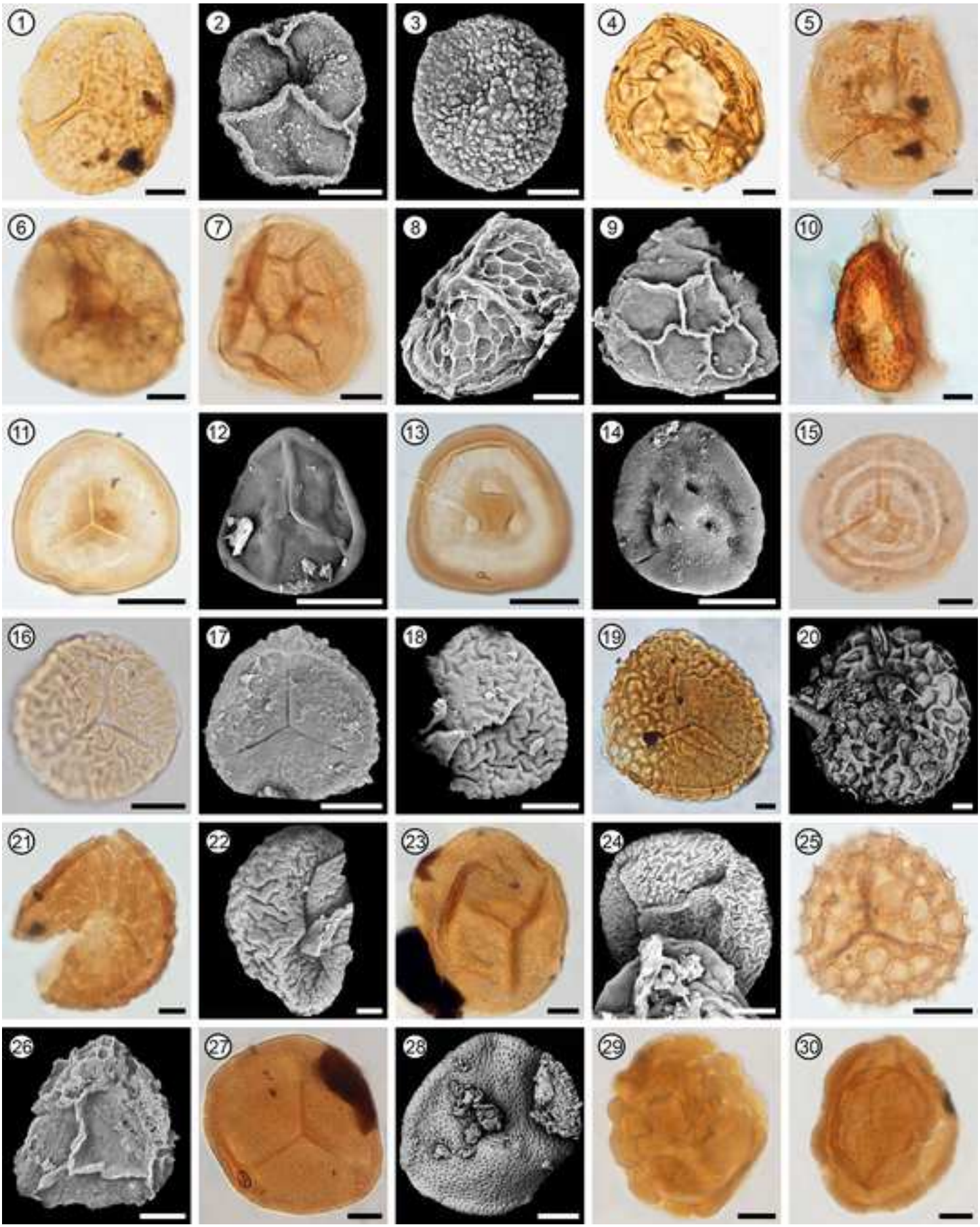

Plate II

Click here to access/download;Figure;Plate II.tif

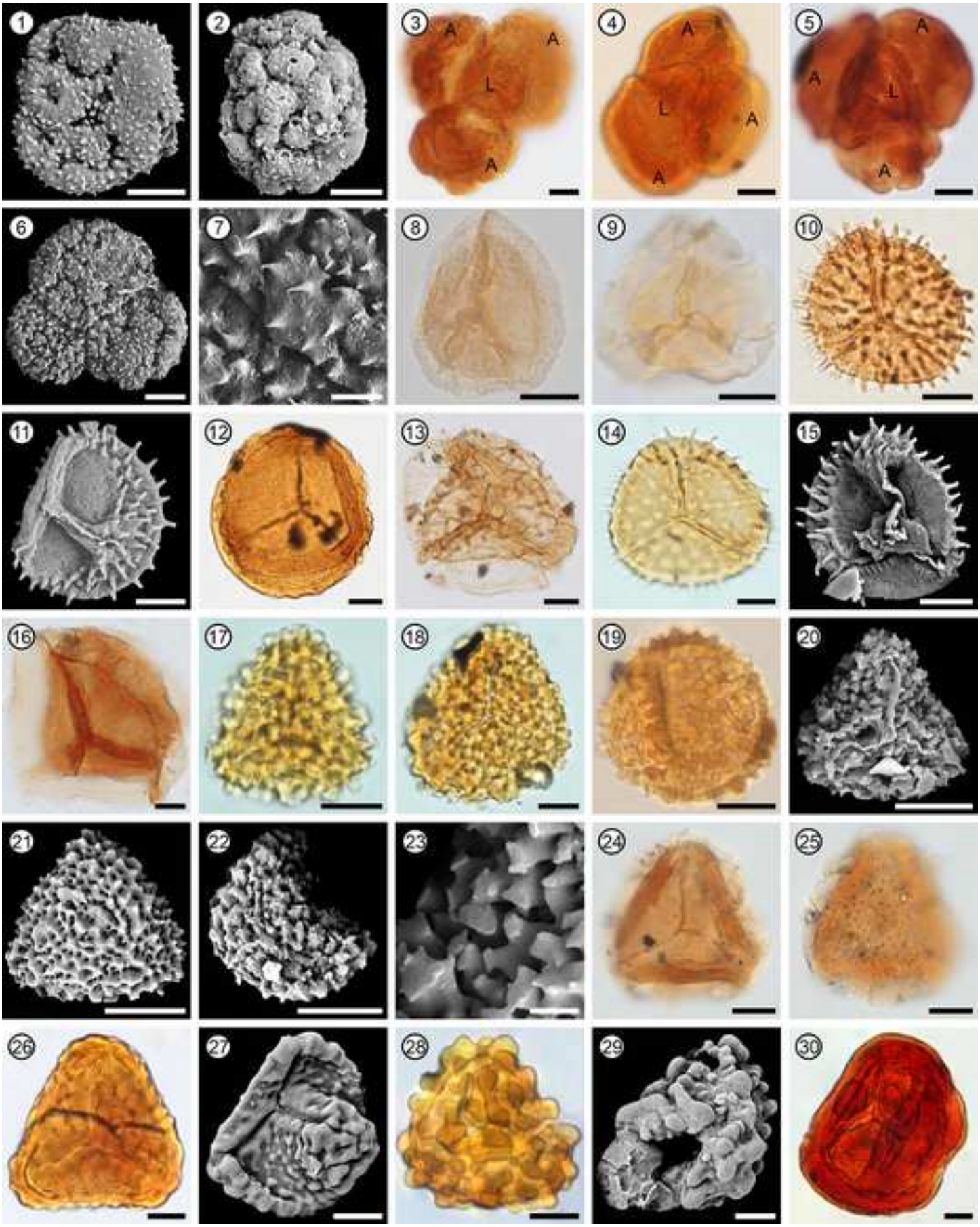

Plate III

Click here to access/download;Figure;Plate III.tif

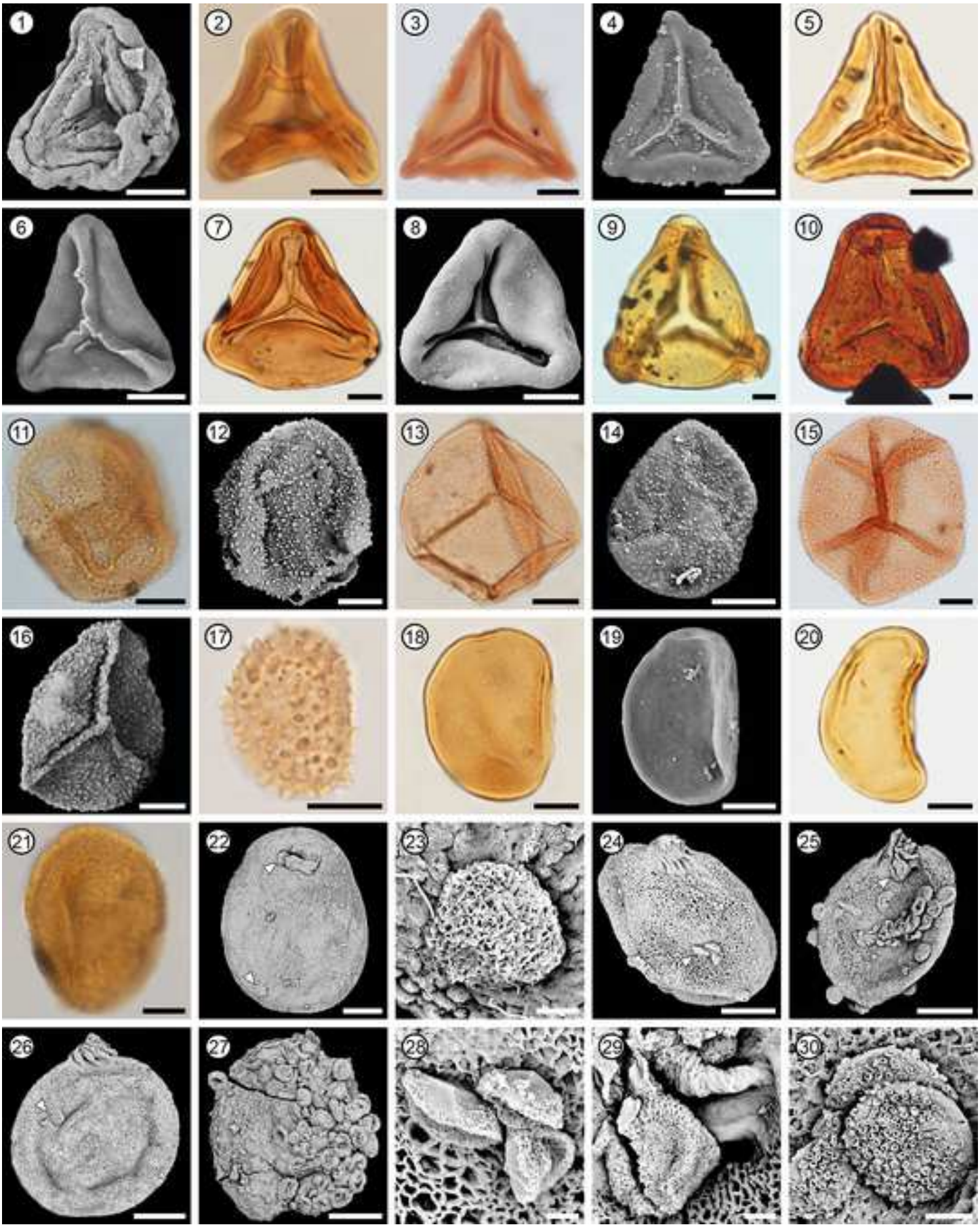

Plate IV

Click here to access/download;Figure;Plate IV.tif

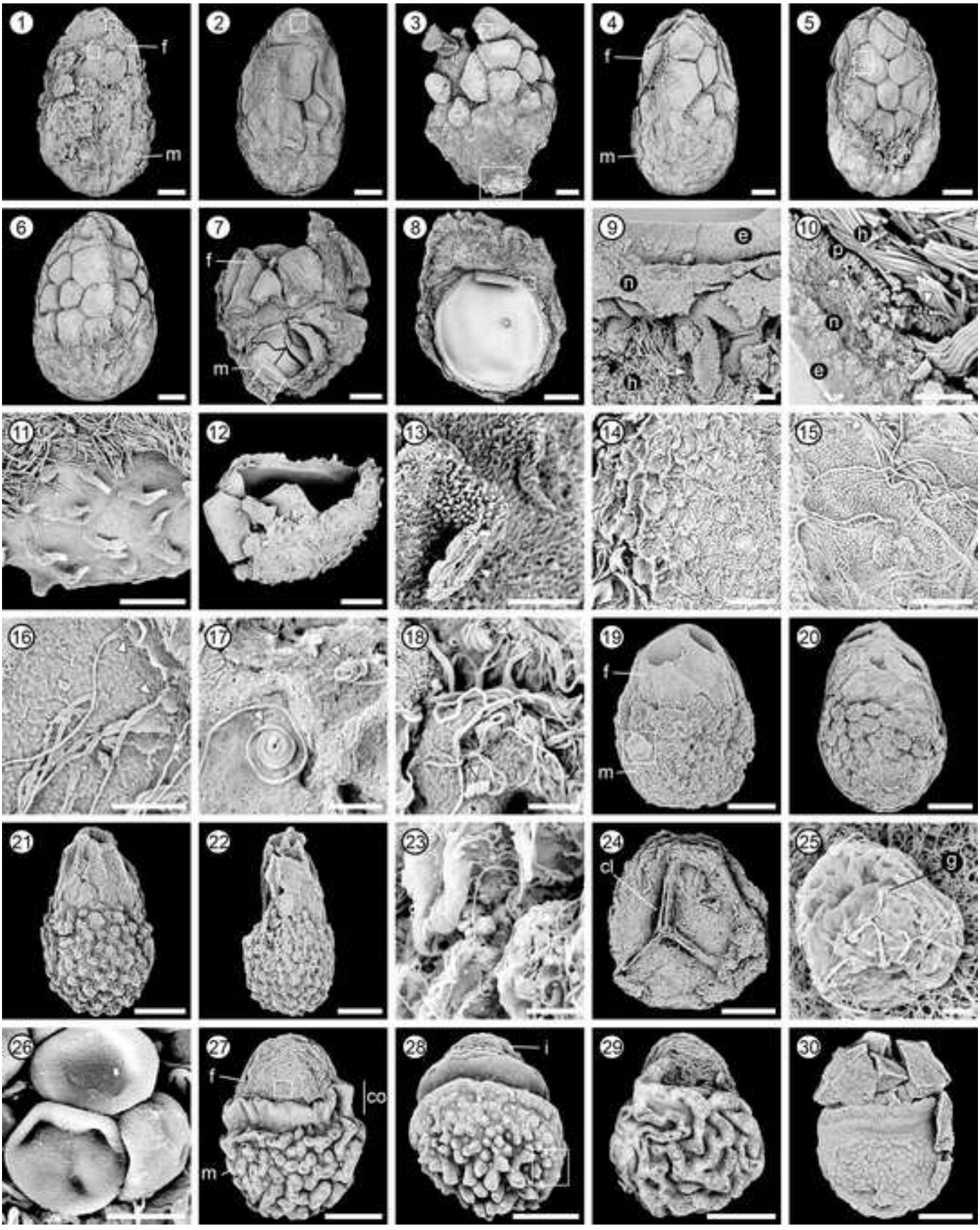

Plate V

Click here to access/download;Figure;Plate V.tif

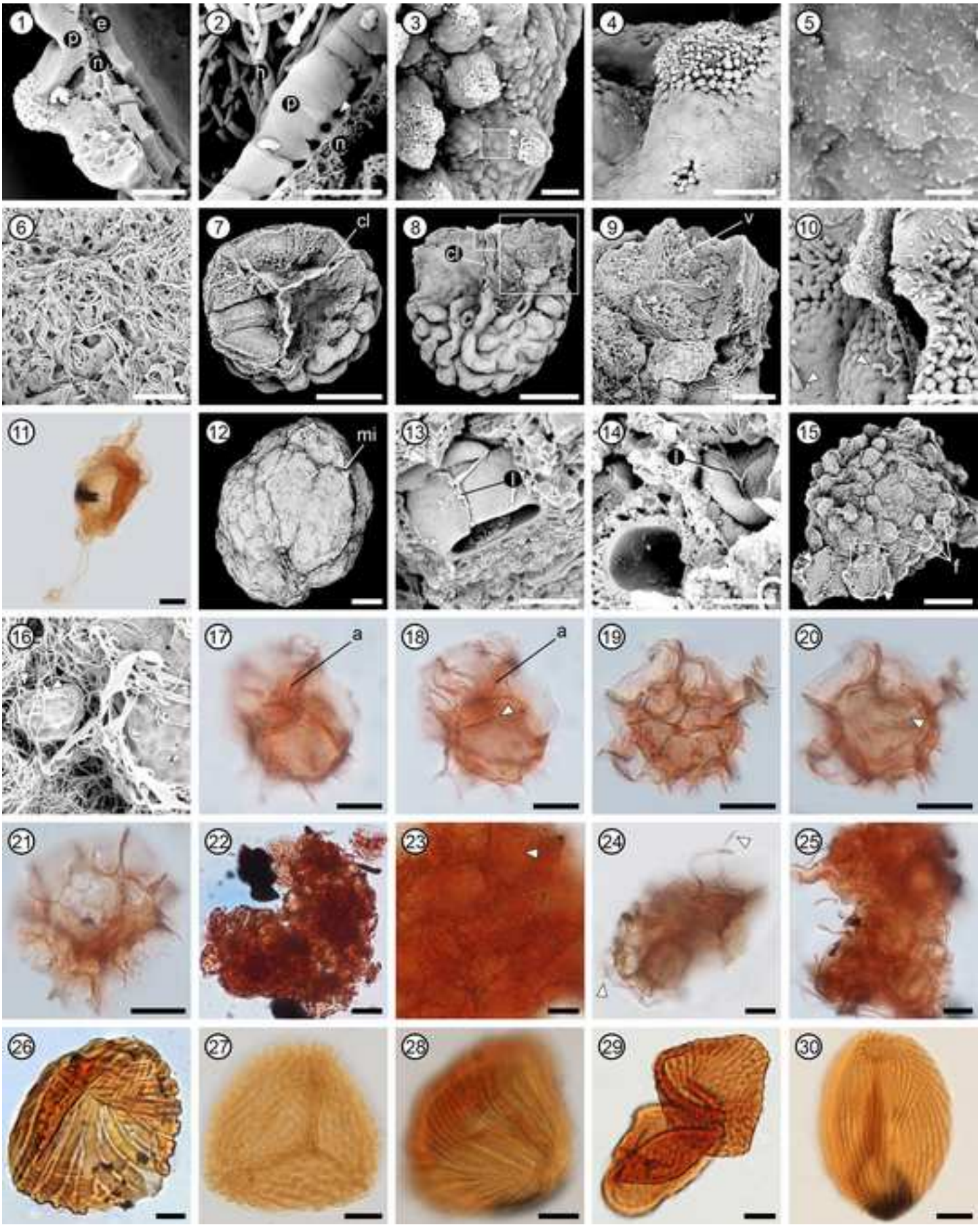

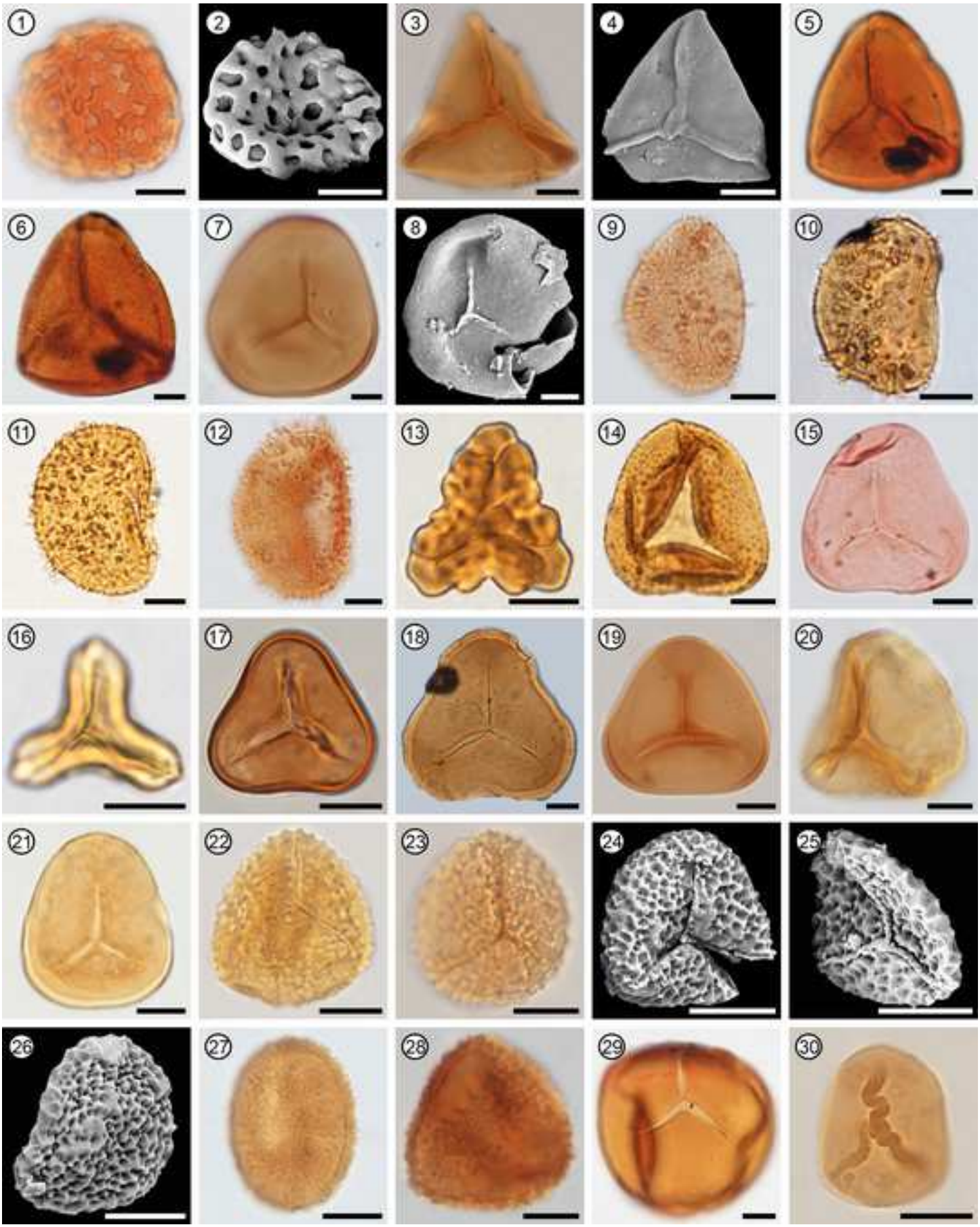

Table (Editable version)

Botanical affinity	Taxa[1]	Illustration	Sections[2]				Maast.	Dan.
			QH/CI	CBO	CBN	CHM		
BRYOPHYTES								
HORNWORTS								
Notothylas breutelii / *Phymatoceros bulbiculosus*	*Foraminisporis dailyi* (Cookson & Dettmann) Dettmann 1963	Pl. I, 1–3	x	x	x	x	x	x
LIVERWORTS								
RICCIACEAE *Riccia*	*Reboulisporites fuegiensis* Zamaloa & Romero 1990	Pl. I, 4	–	x	–	–	x	–
Riccia	*Zlivisporis asper* (Srivastava) comb. nov.	Pl. I, 5	–	x	x	–	x	x
Riccia	*Zlivisporis reticulatus* (Pocock) Pacltová & Simoncsics 1970	Pl. I, 6–9	x	x	x	x	x	x
RIELLACEAE *Riella*	*Aequitriradites spinulosus* (Cookson & Dettmann) Cookson & Dettmann 1961	Pl. I, 10	–	x	x	–	x	–
MOSSES								
SPHAGNACEAE *Sphagnum*	*Cingutriletes australis* (Cookson) Archangelsky 1972	Pl. I, 11, 12	x	x	x	x	x	x
Sphagnum	*Tripunctisporis maastrichtiensis* (Krutzsch) Herngreen et al. 1986	Pl. I, 13, 14	x	x	x	–	x	x
INCERTAE SEDIS								
	Taurocusporites segmentatus Stover 1962	Pl. I, 15	x	x	x	–	x	–
LYCOPHYTES								
LYCOPODIACEAE								
Palhinhaea cernua / *Lycopodiella*	*Camarozonosporites ambigens* (Fradkina) Playford 1971	Pl. I, 16–18	x	x	x	x	x	x
P. cernua / *Lycopodiella*	*Camarozonosporites amplus* (Stanley) Dettmann & Playford 1968	Pl. I, 19, 20	–	x	x	x	x	x
P. cernua / *Lycopodiella*	*Camarozonosporites* sp. 1	Pl. I, 21, 22	–	x	x	x	x	x
	Latrobosporites sp. cf. *L. marginis* Mildenhall & Pocknall 1989	Pl. I, 23, 24	–	–	x	–	x	–
Austrolycopodium paniculatum	*Retitriletes eminulus* (Dettmann) Srivastava 1975	Pl. I, 25, 26	x	x	x	x	x	x
Lycopodium manii, L. laterale / *Huperzia* / *Phylloglossum*	*Sestrosporites pseudoalveolatus* (Couper) Dettmann 1963	Pl. I, 27, 28	–	x	x	–	x	x
SELAGINELLACEAE								
Selaginella	*Acylomorus silviae* Perez Loinaze et al. 2023 / *Lusatisporis choiols* Perez Loinaze et al. 2023	Pl. I, 29, 30; Pl. II, 1–8	x	x	x	x	x	x
Selaginella fusca	*Lusatisporis perinatus* Krutzsch 1963	Pl. II, 9	–	x	x	–	x	x
LYCOP. / SELAG.								
Selaginella latifrons / *Lycopodium deuterodensum*	*Ceratosporites equalis* Cookson & Dettmann 1958	Pl. II, 10, 11	–	x	x	–	x	x
	Densoisporites velatus Weyland & Krieger emend. Krasnova 1961	Pl. II, 12	–	x	x	–	x	x
Lycopodium volubile / *Selaginella*	*Evansispora lacerata* (Norris) Raine 2008	Pl. II, 13	–	x	x	–	x	–
Selaginella tenuispinulosa / *Lycopodium deuterodensum*	*Herkosporites elliottii* Stover 1973	Pl. II, 14, 15	–	x	x	–	x	x
Lycopodium volubile / *Selaginella*	*Kraeuselisporites alexii* Raine 2008	Pl. II, 16	–	x	x	–	x	–
Lycopodium / *Selaginella*	***Neoraistrickia loconiensis***	Pl. II, 17–23	x	x	x	x	x	x
Lycopodium volubile / *Selaginella*	*Perotrilites papillatus* (Harris) Raine 2008	Pl. II, 24, 25	x	x	x	–	x	x
FERNS								
Order CYATHEALES								
CIBOTIACEAE / DICKSONIACEAE	*Cibotiidites auriculatus* Archangelsky & Villar de Seoane 1998	Pl. II, 26, 27	x	x	x	x	x	x
DICKSONIACEAE *Dicksonia squarrosa*	*Cibotiidites tuberculiformis* (Cookson) Skarby 1974	Pl. II, 28, 29	x	x	x	x	x	x

Lophosoria quadripinnata	*Cyatheacidites annulatus* Cookson ex Potonié 1956	Pl. II, 30; Pl. III, 1	x	x	x	x	x	x
Order GLEICHENIALES								
DIPTERIDACEAE *Cheiropleuria*	*Cibotiumspora jurienensis* (Balme) Filatoff 1975	Pl. III, 2	x	x	x	x	x	x
GLEICHENIACEAE *Dicranopteris*	*Clavifera triplex* (Bolkhovitina) Bolkhovitina 1966	Pl. III, 3, 4	x	x	x	x	x	x
Gleichenia	*Gleicheniidites senonicus* Ross 1949 emend. Skarby 1964	Pl. III, 5, 6	x	x	x	x	x	x
MATONIACEAE / DIPTER.	*Dictyophyllidites harrisii* Couper 1958	Pl. III, 7, 8	x	x	x	x	x	x
	Matonisporites phlebopteroides Couper 1958	Pl. III, 9	–	x	x	x	x	x
	Phlebopterisporites equiexinus (Couper) Juhász 1979	Pl. III, 10	–	x	x	x	x	–
Order OSMUNDALES								
OSMUNDACEAE	*Baculatisporites comaumensis* (Cookson) Potonié 1956	Pl. III, 11, 12	–	–	x	x	x	x
	Osmundacidites diazii Volkheimer 1972	Pl. III, 13, 14	x	x	x	x	x	x
	Osmundacidites sp. 1	Pl. III, 15, 16	x	x	x	x	x	x
Order POLYPODIALES								
CYSTOPTERIDACEAE *Cystopteris*	*Tuberculatosporites parvus* Archangelsky 1972	Pl. III, 17	–	x	x	x	x	x
POLYPODIACEAE	*Laevigatosporites ovatus* Wilson & Webster 1946	Pl. III, 18, 19	x	x	x	x	x	x
	Laevigatosporites sp. 1	Pl. III, 20	x	x	x	–	x	–
	Polypodiidites speciosus (Harris) Archangelsky 1972	Pl. III, 21	x	x	x	x	x	x
Order SALVINIALES								
MARSILEACEAE *Regnellidium*	*Molaspora lobata* (Dijkstra) Hall, in Hall & Peake 1968 / *Crybelosporites pannuceus* (Brenner) Srivastava 1977 (M / m)	Pl. III, 22, 23	x/x	x/x	x/x	x/x	x/x	–/x
	Molaspora reticulata Campbell & Untergasser 1972 / *Gabonisporis cristata* (Stanley 1965) Sweet 1986 (M / m)	Pl. III, 24–30	–/x	x/x	x/x	x/x	x/x	–/x
SALVINIACEAE *Azolla*	*Azolla andreisii* De Benedetti & Zamaloa 2021 / *Azolla* sp. 1? (M / m)	Pl. IV, 1–18	–/–	x/x	x/x	–/x	x/x	–/x
	Azolla coloniensis De Benedetti & Zamaloa emend. Hermsen et al. 2019 (M / m)	Pl. IV, 19–26	x/x	x/x	x/x	x/x	x/x	–/x
	Azolla sp. cf. *A. keuja* Jud et al. 2019	Pl. IV, 27–30; Pl. V, 1–10	–	–	x	–	x	–
INCERTAE SEDIS	*Ariadnaesporites micromedusus* Stough 1968	Pl. V, 11	–	–	–	x	x	–
	Azollopsis intermedia Sweet & Hills 1974 (M / m)	Pl. V, 12–14	–/x	x/x	x/x	–/x	x/x	–/–
	Azollopsis tomentosa Hall 1968 (M / m)	Pl. V, 15, 16	–/x	x/x	x/x	–/x	x/x	–/–
	Ghoshispora sp.	–	–	–	x	–	x	–
	Grapnelispora loncochensis Papú 1997	–	–	x	x	x	x	x
	Paleoazolla patagonica Archangelsky et al. emend. De Benedetti & Zamaloa 2020 (M / m)	–	x/x	x/x	x/x	–/x	x/x	–/–
	Thecaspora polygonalis	Pl. V, 17–23	x	x	x	x	x	x
	Genus et species indet.	Pl. V, 24, 25	–	–	x	–	x	–
Order SCHIZAEALES								
ANEMIACEAE *Anemia*	*Palaeomohria patagonica* Archangelsky 2009	Pl. V, 26	–	x	x	–	x	–
ANEMIACEAE / SCHIZAEACEAE	*Cicatricosisporites ornatus* Srivastava 1972	Pl. V, 27	–	–	x	–	–	x
	Cicatricosisporites sp. 1	Pl. V, 28	x	x	x	x	x	x
	Cicatricosisporites sp. 2	Pl. V, 29	–	x	x	–	x	–
	Cicatricososporites eocenicus (Selling) Jansonius and Hills 1976	Pl. V, 30	–	x	x	–	x	x

LYGODIACEAE *Lygodium*	*Klukisporites pseudoreticulatus* Couper 1958	Pl. VI, 1, 2	x	x	x	x	x	x
Order *INCERTAE SEDIS*								
HYM. / SCHIZ. / OSM.?	*Biretisporites crassilabratus* Archangelsky 1972	Pl. VI, 3, 4	x	x	x	–	x	x
	Biretisporites sp. 1	Pl. VI, 5, 6	–	x	x	–	x	–
	Biretisporites sp. 2	Pl. VI, 7, 8	–	x	x	–	x	x
	Clavatosporis varians	Pl. VI, 9–12	x	x	x	x	x	x
	Concavisporites sp. cf. *C.* sp. 2 of Archangelsky 1972	Pl. VI, 13	–	–	x	–	x	–
SCHIZ. / DICKS. / CYAT.?	*Concavissimisporites verrucosus* Delcourt & Sprumont emend. McKellar 1998	Pl. VI, 14	–	x	x	–	x	x
DICKS. / CYAT.?	*Cyathidites australis* Couper 1953	Pl. VI, 15	x	x	x	x	x	x
DICKS. / CYAT.?	*Cyathidites concavus* (Bolkhovitina) Dettmann 1963	Pl. VI, 16	x	x	x	x	x	x
DICKS. / CYAT./DENNST.?	*Cyathidites minor* Couper 1953	Pl. VI, 17	x	x	x	x	x	x
DICKS. / CYAT.?	*Cyathidites patagonicus* Archangelsky 1972	Pl. VI, 18	x	x	x	x	x	x
CYAT. / DICKS.?	*Deltoidospora* sp.	Pl. VI, 19	–	x	x	–	x	x
	Granulatisporites sp.	Pl. VI, 20	–	–	x	–	x	x
CYAT. / PTERID.?	*Leiotriletes regularis* (Pflug) Krutzsch 1959	Pl. VI, 21	x	x	x	–	x	x
	Microreticulatisporites patagonicus	Pl. VI, 22–26	x	x	x	x	x	x
	Peromonolites vellosus Partridge 1973	Pl. VI, 27	x	–	x	x	x	x
	Rugulatisporites sp.	Pl. VI, 28	–	x	x	–	x	x
	Todisporites major Couper 1958	Pl. VI, 29	–	x	x	–	x	–
	Undulatisporites sinuosis Groot & Groot 1962	Pl. VI, 30	–	x	x	–	x	x

[1] New species are in bold.

[2] Stratigraphic sections: QH/CI (Quebrada del Helecho/Cañadón del Irupé), CBO (Cerro Bosta), CBN (Cerro Buitre Norte), and CHM (Chiva Muerta). Presence (x); Absence (–).

(M / m): M = megaspore; m = microspore or microspore massulae.